Spiecker Barbara J (Orcid ID: 0000-0002-6895-9424)
Menge Bruce A. (Orcid ID: 0000-0002-2981-9517)

Journal: Ecological Monographs

Manuscript type: Article

El Niño and marine heatwaves: Ecological impacts on Oregon rocky intertidal kelp communities at local to regional scales

Barbara J. Spiecker[1] and Bruce A. Menge[1]

[1]Department of Integrative Biology, Oregon State University, Corvallis, OR, USA 97331.

Corresponding Author: Barbara J. Spiecker. E-mail: barbara.spiecker@gmail.com

Manuscript received 3 March 2021; revised 17 July 2021; accepted 3 September 2021.

Handling Editor: Michael H. Graham

Open Research: Data (Spiecker and Menge 2021) are available from Dryad:

https://doi.org/10.25349/D9360J

Abstract

El Niños and marine heatwaves are predicted to increase in frequency under greenhouse warming. The impact of climate oscillations like El Niño-Southern Oscillation on coastal environments in the short-term likely mimics those of climate change in the long-term; therefore, El Niños may serve as a short-term proxy for possible long-term ecological responses to an increasingly variable climate. Understanding and prediction of ecosystem responses requires elucidating the mechanisms underlying different organizational scales (organism, space, and time). We analyzed spatiotemporal variation in the effect of the 2015-16 El Niño and the overlapping 2014-2016 East Pacific marine heatwave on three intertidal kelps (*Hedophyllum sessile, Egregia menziesii,* and *Postelsia palmaeformis)* at 7 sites across 300 km of the Oregon coast and over three years post El Niño. We measured percent cover, density, maximum length, growth, and Carbon:Nitrogen (C:N) ratios monthly in spring/summer at each site from 2016 through 2018. Results revealed a complex interplay between spatial, temporal, and biological factors that modified the effects of these thermal anomalies on Oregon intertidal kelp populations. Our findings generally agree with prior literature showing detrimental effects of El Niño on kelp. However, El Niño and possibly marine heatwave effects can be mitigated or amplified by environmental processes and kelp life history strategies. In our study, coastal upwelling provided regional relief for the kelp individuals with respect to their growth needs and mitigated the adverse effects of warming. On the other hand, we also found that coastal upwelling amplified, or compounded, detrimental effects of El Niño by increasing phytoplankton-induced shading and mollusk grazing on juvenile and adult kelps, thereby reducing their density. Given the greater uncertainty associated with warming events and climate

change in the California Current Upwelling System and its biological implications, our findings reiterate the importance of acquiring better understanding of how context-specific underlying conditions modify ecosystem processes. More specifically, understanding how demographic traits and life history stages of kelp change with biological interactions and environmental forcing over temporal and spatial scales is crucial to anticipating future climate change ramifications.

Key words: coastal upwelling; El Niño; ENSO; kelp populations; life history stage; marine heatwaves; Oregon shores; rocky intertidal; spatial scale; temporal scale

Introduction

Macroalgal communities are shaped by the complex interplay of a multitude of external biotic and abiotic factors and the intrinsic responses of the individual macroalgal species (Dayton 1985, Dayton et al. 1984, 1992, 1999, Schiel and Foster 2006, 2015). These factors are not stable over space or time, especially in the context of climate change. Tolerance levels are species-, life history stage-, or even specimen-specific. As stated by Davison and Pearson (1996), "stress must be defined in terms of the response of an individual rather than the value of a particular environmental variable."

Environmental factors drive the formation of upper and lower threshold values of tolerance of all species including macroalgae (van den Hoek 1982). Kelps are among the most spatially extensive and abundant of the macroalgae, and thus are critical to the sensitivity of algae-dominated systems to environmental change. Because of tolerance boundaries, kelps

continuously optimize trade-offs between demographic traits of growth, reproduction, and survival throughout their life history. Most ecological studies have focused on the large sporophyte stage of kelp species (Dayton 1985), often with an implicit assumption that the growth and survival of juvenile kelps were determined by the same environmental factors that influence the adult sporophytes. However, more recent work emphasizes the different threshold factors critical to the separate life-history stages, especially the gametophyte and juvenile stages (Schiel and Foster 2006, Schiel and Foster 2015).

Important environmental factors influencing kelp communities include light, temperature, nutrients, grazing, and sedimentation. The relative importance of these factors may differ between adult and juvenile kelp stages (Dayton 1985). Specifically, **(1) Light:** Irradiance quality and quantity is critical to all kelp life-history stages, and many important physical and biological processes are ultimately light-related. Factors affecting irradiance may include suspended sediments, phytoplankton blooms, and shading by algal canopies (Schiel and Foster 2015). Some adult kelps are generally insensitive to changes in subsurface light because they form a surface canopy and can translocate the products of photosynthesis toward the holdfast, while light levels to the seafloor are frequently below those needed for the growth of juvenile sporophytes (Neushul 1981, Dean and Jacobsen 1984, Reed and Foster 1984). **(2) Temperature:** It is challenging to isolate temperature effects from many other environmental factors in field conditions. For example, light and nutrient thresholds depend on ambient temperature (Mann 1971, Lüning 1980, Dean and Jacobsen 1984, Dean and Jacobsen 1986). However, under controlled laboratory conditions, increasing temperature negatively affected both adults and juveniles (Schiel and Foster 2006, Hollarsmith et al. 2020). **(3) Nutrients:** The evidence emphasizes the importance of dissolved nitrogen for kelps (Schiel and Foster 2015).

Experimental fertilization of kelps with nitrate has dramatically enhanced growth (DeBoer 1981, North 1983, Dean and Jacobsen 1986). **(4) Grazing:** Young and old macroalgal tissues often have different palatability or anti-grazing characteristics, and suffer different grazing pressures. Grazers, such as snails, limpets, chitons, sea urchins, and fish usually preferentially graze on juvenile kelps over adults (Watson and Norton 1985, Van Alstyne et al. 1999, Van Alstyne et al. 2001, Taylor et al. 2002, Heaven and Scrosati 2004, Taylor and Schiel 2010). **(5) Sedimentation:** Sedimentation and sediment scour are highly detrimental to kelps (Dean and Deysher 1983, Dayton et al. 1984). In most cases, their effects are most severe on spores, gametophytes, and juvenile sporophytes (Dayton et al. 1984).

The intrinsic responses of kelps to environmental change vary with life history stage. Variation in demographic traits can be explained by stress or reduced growth (or other integrative parameters such as reproduction and recruitment) driven by limited resources (Schiel and Foster 2006, Schiel and Foster 2015). Resource limitation and physiological performance are the principal determinants of kelp tolerance to environmental variability and change. As climate or other environmental conditions shift, responses are initially based on adaptations molded through kelp evolutionary history. Physiological adaptations and environmental variables do not change independently in nature, and may often covary as a reflection of mesoscale or global scale events (Phillips and Pérez-Ramirez 2017). One of these events is El Niño-Southern Oscillation (ENSO), which in addition to altering physico-chemical environmental properties, can also cause severe ecological impacts.

ENSO is a major ecological process governing the dynamics of kelp populations (e.g., Graham et al. 1997, Dayton et al. 1999, Parnell et al. 2010). Warm phase El Niño effects are multi-faceted, reducing nutrients, intensifying wave action (contributing to changes in light and

sedimentation), elevating sea temperature, and raising sea level, especially in the East Pacific (Philander 1983, Ebeling et al. 1985, Tegner and Dayton 1987). ENSOs can also have dramatic effects on species interactions and the structuring of communities. Although El Niño impacts on marine life typically are strongest in the equatorial Pacific, its effects can propagate north and south along the coast of the Americas, affecting marine life across a vast geographic range. For example, El Niño caused declines in multiple macroalgal species in the equatorial Galapagos Islands (Vinueza et al. 2006), led to declines of 50-70% in California kelp populations (Dayton et al. 1992), and severely reduced growth and abundance of Oregon intertidal kelps (Freidenburg 2002). However, the detrimental effects of El Niños can be mitigated by strong and persistent coastal upwelling. Studies show that in the California Current Upwelling System (CCUS), kelps were able to recover quickly or maintain their population densities due to upwelling-driven inputs of nutrients (Dayton et al. 1992, Freidenburg 2002).

Despite considerable progress in our understanding of the impact of climate change on many oceanographic processes, earlier research reached no clear consensus across the generalized circulation models on El Niño intensities or frequencies in response to carbon dioxide increases (Collins 2000, Guilyardi 2006, Meehl et al. 2006, Merryfield 2006, Cherchi et al. 2008). A review of these models found projections anywhere between 30% decreases to 30% increases in ENSO-driven sea surface temperature variability (Vecchi and Wittenberg 2010). However, Cai et al. (2018) recently pointed out that the "no consensus" conclusion (i.e., predicted ENSO patterns greatly differed from one model to another) resulted from using spatially fixed sea surface temperatures (SST) and not incorporating nonlinearities of associated ENSO processes. After correcting these issues, Cai et al. (2018) found a robust increase in future

SST variability among CMIP5 climate models. An increase in SST variance implies an increase in the frequency of 'strong' El Niño events and associated extreme weather events.

ENSOs have been recently joined by the novel rise of marine heatwaves (MHWs), which can impose severe direct thermal stresses on organisms and thus lead to a variety of indirect effects. MHWs with notable ecological impacts have been occurring more frequently in the past century as a result of global warming (Bindoff et al. 2013, Oliver et al. 2018). MHWs are defined by prolonged periods of anomalously warm ocean temperatures (Hobday et al. 2016). They can overlap or coincide with El Niño events, thus compounding devastating and long-lasting thermal impacts on marine ecosystems (Filbee-Dexter et al. 2020, Gupta et al. 2020). Like El Niños, MHWs dramatically reduce kelp populations and can trigger complete regime shifts from kelp forests to seaweed turfs (Wernberg et al. 2016) or sea urchin barrens (Rogers-Bennett and Catton 2019).

In addition to causing anomalously high and persistent sea surface temperatures, these thermal events may cause extreme weather patterns (i.e., persistent high air temperature and droughts) with severe effects. For example, in the northwest Iberian peninsula, Román et al. (2020) found that air temperature was a critical factor in determining physiological performance and survivorship of intertidal canopy-forming macroalgae while high sea temperature had sublethal effects. Some intertidal macroalgae experienced decreases in maximum quantum yield (Fv/Fm), growth and high mortality when exposed to higher air temperatures during the emersion periods. In another example, Thomsen et al. (2019) found that MHWs caused high mortality of *Durvillaea* spp. on the New Zealand coast.

Environmental factors associated with climate change and ENSO that are important to juvenile and adult kelps are predicted to intensify (IPCC 2018). The multifarious nature of

environmental change and species-specific properties of kelps could create a major obstacle in developing accurate predictions about biological responses to climate change in marine habitats, especially in the rocky intertidal of the CCUS. Rocky intertidal habitats are ecotonal, with marine and terrestrial influences, both being altered by climate change (Sagarin et al. 1999, Harley et al. 2006, Doney et al. 2012, Howard et al. 2013). Hence, organisms in this ecosystem are subject to aquatic and aerial environmental challenges (Helmuth et al. 2006). Survival, growth, and reproduction of important habitat forming rocky-shore kelps are known to vary with climatically sensitive environmental variables (Davison and Pearson 1996, Harley et al. 2012). However, our understanding of the relationship between environmental change and the performance of individual kelp species in a community setting is limited. We need more studies that consider ecological performance of kelps within the context of changing environmental regimes, and delineate how the performance of each species vary across life stages and demographic traits.

Ecologists use several common quantitative metrics (percent cover, density, and size of an individual) to characterize community structure and measure changes in community composition and species abundance across space and time. Since these metrics are not necessarily correlated, a closer look at the types of information each metric yields is necessary to fully assess responses of the macroalgal species to environmental change. Do these metrics assess overall changes within a species and a community as a whole and/or do they assess how intrinsic properties of a species change in response to external stimuli? What kind of insights will these metrics reveal or mask?

We addressed these issues by investigating the responses of three common intertidal kelp species at seven locations along the Oregon coast. This ecosystem is an excellent natural

laboratory for investigating the role of environmental and biological processes in shaping the intertidal kelp communities due to its documented ecological repercussions from El Niño and its exposure to strong environmental gradients (i.e., coastal upwelling, variable wave action, emergence time during low tide) over short spatial scales (Freidenburg 2002, Menge et al. 2015). To better understand the ecological controls that modulate the effects of El Niños on the Oregon rocky intertidal kelp populations across various organizational scales (organism, space and time), we asked the questions and pose the hypotheses below:

- **Q1:** What were the temporal response patterns of three common intertidal kelps after the 2014-2016 thermal events?
    - **H1:** As was observed after the 1997-98 El Niño, kelp metrics would be the lowest immediately after the event and increase over time.

- **Q2:** Were there spatial differences in the response patterns of three common intertidal kelps?
    - **H2:** Relative performances of kelps would vary strongly in space, with lower performance at the northern and central Oregon regions and higher performance in southern Oregon due to upwelling variation.

- **Q3:** Which environmental parameters had the strongest relationship with the response patterns of three common intertidal kelps?

- **H3:** Kelp metrics would respond positively over the years and the rate of responses would be the fastest where dissolved inorganic nitrogen is most abundant.

- **Q4:** Would the ecological metrics quantified (percent cover, density, and length of an individual) for all three species vary uniformly or vary by taxon?
  - **H4:** Due life-history related conservatism, the metrics would vary by taxon.

Methods

Study System

We studied three common intertidal kelp species (*Hedophyllum sessile, Postelsia palmaeformis,* and *Egregia menziesii*) along 300 km of the Oregon coast. Survey sites were nested within each of three capes or regions (from North to South): Cape Foulweather [Fogarty Creek, Boiler Bay, Depoe Bay], Cape Perpetua [Yachats Beach and Strawberry Hill], and Cape Blanco [Cape Blanco North and Rocky Point] (Appendix S1: Table S1; Fig. 1). The sea palm *P. palmaeformis* was mostly absent at Boiler Bay, so we added sea palm studies at Depoe Bay (South Point) as our second replicate site for this species. All aspects of the study: surveys, growth, density, and Carbon:Nitrogen (C:N) ratios were conducted monthly in spring/summer, when growth and reproduction occur, at each site from 2016 through 2018 (Spiecker and Menge 2021).

Each cape has different physical, biological, and geological features (Menge et al. 2015). Cape Foulweather has a relatively narrow continental shelf with stronger offshore flow, experiences more intermittent upwelling, has high dissolved inorganic nitrogen levels, and is dominated by macrophytes (kelp, surfgrass, and other macroalgae) in the low intertidal zone. Cape Perpetua has a wider continental shelf that generates weak and retentive currents, experiences more intermittent upwelling, has lower dissolved inorganic nitrogen and higher phytoplankton levels, and is dominated by sessile invertebrates and non-canopy and turf-forming algae in the low intertidal zone. Cape Blanco has a narrow continental shelf with a strong offshore jet, experiences more persistent upwelling, has higher dissolved inorganic nitrogen levels, and is dominated by macrophytes in the low intertidal zone.

Macroalgal Transect Surveys

We used transect surveys to examine changes in algal abundance and size across capes. At each site, we established five permanent (5 x 1 m) plots for each species. Since our goal was to document kelp performance and not characterize species populations at the site scale, plots were placed where the target species were most abundant. Further, sampling the same marked plots is in our view the best way to document temporal change. Plots were sampled using 0.5 x 0.5 m^2 quadrats placed contiguously on both sides of a transect line run through the middle of the plot along the 5 m axis. Data collected monthly for each species were kelp percent cover, density, and maximum length of the longest individual in each quadrat, or for *P. palmaeformis*, maximum stipe and frond length (Appendix S1: Table S2).

***In situ* Macroalgal Growth and Breakage**

We quantified growth of *H. sessile* and *E. menziesii* only through elongation of their blades because their growth with respect to the thickening of stipe, blade, and holdfast tissues are trivial compared to blade elongation, thus resulting in negligible short-term changes. We did not quantify *P. palmaeformis* growth because of their complex growth patterns and high breakage rate. The sea palm grows in two directions at a similar rate: (1) elongation of blades from the meristematic region, and (2) elongation and thickening of the stipe from the meristoderm beneath the cortex (Holbrook 1991). Because of this complexity, there was no straightforward and non-intrusive way to measure growth in the field. Additionally, their high breakage rate (as a result of wave exposure) made it difficult to track individuals for growth rate measurements.

For *H. sessile* and *E. menziesii*, growth rates were quantified using the hole-punch method (Kain 1976, Larkum 1986). Monthly *H. sessile* growth rate was quantified by punching a hole in the longest vegetative blade of each individual 5 cm above the meristematic region. Growth was measured as the distance between the base of the blade and the hole which moves away from the holdfast as the blade grows. Monthly *E. menziesii* growth rate was determined by punching a hole in the longest vegetative blade 5 cm below the intercalary meristematic region. Growth was measured as the distance between the meristematic region and the previous hole (Appendix S1: Table S2). Twenty individuals of each species per site were identified using coded plastic tags attached to the substrate adjacent to each alga with a stainless-steel lag screw placed in pre-drilled holes in the rock.

Using the same individuals tagged for growth measurements, we also quantified percent rachis breakage of *E. menziesii.* Individuals lacking a rachis beyond the site of the hole punch

(for the growth measurement) was recorded as "broken." Percent rachis breakage was calculated by dividing the number of "broken" individuals by the total number of the tagged individuals. *H. sessile* experienced no blade breakage throughout the survey obviating the need for its estimation.

Elemental Composition

Elemental composition provides a measure of kelp performance with regard to nutrient uptake. To identify biogeographic patterns of elemental composition (%C, %N, and C:N), we quantified the Carbon:Nitrogen ratio (C:N; Appendix S1: Table S2) for each species. We randomly collected samples from twenty separate individuals of each species: one-inch square sections of *H. sessile* blades, five fronds of *P. palmaeformis* and 5-cm sections of *E. menziesii* terminal blades. All samples were placed in plastic zip-top bags in the field, kept cool, and subsequently stored in a –20°C freezer.

Samples for the C:N analysis were prepared by thawing at room temperature and removal of epiphytes and fouling organisms. Samples were rinsed with deionized water and dried in ashed foil packets at 60°C for 48 hours. They were then ground to a powder using a Spex Sigma Prep 8000D Mixer/Mill, and stored in 2 mL microcentrifuge tubes. Carbon-13 and Nitrogen-15 contents were analyzed by Oregon State University Stable Isotope Lab with a Carlo Erba NA1500 elemental analyzer and a DeltaPlus isotope ratio mass spectrometer. Due to financial constraints, only *H. sessile* samples taken each July from 2016 to 2018 were analyzed.

Environmental Parameters

Environmental data (chlorophyll-a [Chl-a], dissolved inorganic nitrogen [DIN], sea surface temperature [SST], surface air temperature [SAT], Multivariate El Niño Southern Oscillation Index [MEI v2], North Pacific Gyre Oscillation [NPGO], Biologically Effective Upwelling Transport Index [BEUTI], and significant wave height [SWHT]) for the sampling months were provided by the Menge laboratory or the National Oceanic and Atmospheric Administration (NOAA) (Appendix S1: Table S2). Daily SST and SAT were measured at every site using HOBO TIDBIT and/or Pendant temperature loggers (Onset, Bourne, Massachusetts, USA) held to the rock with small stainless-steel cages. The loggers sampled at 5-min intervals in the low intertidal at all sites. A detiding program was used to separate air from water temperatures (Menge et al. 2008). Monthly Chl-a and DIN were extracted from bottle samples taken from the surf zone at every site and measured using the protocol in Menge et al. (1997). Monthly SWHT was measured by NOAA buoys 20 nautical miles west of the Oregon coast at 42°N (Station 46015) and 45°N (Station 46050) latitudes (https://www.ndbc.noaa.gov/). For months when these buoys were inoperative, we used the wave data from the next closest buoy and fitted a regression line to estimate the missing values ($R^2 = 0.82$). BEUTI (Jacox et al. 2018) data were measured offshore between 31°N and 47°N latitudes at 1º resolution (https://oceanview.pfeg.noaa.gov/products/upwelling/intro). MEI v2) data were obtained from NOAA's Physical Sciences Laboratory (https://psl.noaa.gov/enso/mei/) and NPGO data were obtained from Georgia Institute of Technology (Di Lorenzo et al. 2008; http://www.o3d.org/npgo/).

Statistical Analyses

***Species Performance Metrics*:** Statistical analyses were conducted on performance metrics of each species, including percent cover, density, maximum length, growth rate, percent breakage, and elemental composition using R Studio (R Core Team 2017, Version 1.1.456, Package: stats, Function: cor) and SAS Enterprise Guide (SAS Institute Inc. 2013, Version 7.1, Procedure: MIXED, GLIMMIX). These analyses included Hierarchical Linear Mixed Model (HLMM), Hierarchical Generalized Linear Mixed Model (HGLMM), Least Squares Means (LSM), and correlation coefficients. Assumptions appropriate for each model (independence, homoscedasticity, and normality) were examined visually and all data met the criteria. Corrections were not applied for multiple pairwise comparisons because the contrasts were planned *a priori* with the intention of comparing the observational results with prior results in the literature. Furthermore, reducing the type I error for null associations may increase the type II error for those associations that are not null, which is a concern when important differences may be deemed non-significant (Feise 2002, Perneger 1998, Rothman 1990). Thus, instead of applying corrections, precise p-value and standard error were reported.

***Response Trajectories*:** The species matrix (162 spatiotemporal sampling units x 9 species performance measures) contained percent cover, density, and maximum length of the three species over three months (May, June, July) and three years (2016, 2017, 2018). To make analyses more manageable, replicates (quadrats, transects, and sites) were aggregated and averaged to acquire a single response value for each species performance in each cape, month, and year, thus reducing the dimensions of the species matrix to 27 spatiotemporal sampling units

x 9 species performance measures. The environmental matrix (27 spatiotemporal sampling units x 8 environmental variables) contained measurements of environmental variables (Appendix S1: Table S2). All species performances within each spatiotemporal sampling unit were relativized by each species performance maximum to standardize different metrics across the columns.

Non-Metric Multidimensional Scaling (NMDS) was conducted to visualize spatiotemporal sampling units (cape, month, and year) in species performance space. NMDS ordinations used Sorensen distances, had a random starting configuration, did not penalize ties, and were run 200 times with real and randomized data, an instability criterion of 0.00001 and a maximum of 500 iterations. This analysis was conducted using PC-ORD (McCune and Mefford 2016).

Results

Performance and response patterns of each kelp species showed a complex interplay among spatial, temporal, and biological factors (Table 1). To ease understanding, below we will refer to the different regions as the Northern (Cape Foulweather = CF), Central (Cape Perpetua = CP) and Southern Capes (Cape Blanco = CB).

Hedophyllum sessile

H. sessile generally exhibited positive responses in the years following the El Niño event with respect to maximum length, density, percent cover, growth rate and carbon to nitrogen ratio.

However, the rate and direction of these responses varied by site and cape. Furthermore, there was a notable decline in the year 2018 for some of the metrics.

Maximum Length: Maximum length of *H. sessile* varied with cape and year (cape x year interaction; HLMM; F = 20.42, $P < 0.0001$; Appendix S1: Table S3; Fig. 2A, B). Temporally, the average maximum length differed among years (HLMM; F = 129.02, $P < 0.0001$; Appendix S1: Table S3; Fig. 2 A, B). Spatially, *H. sessile* at the Southern Cape (CB) were longer on average than those at the Northern Cape (CF) and were generally of the same length as those at the Central Cape (CP) (LSM; (CB/CF) $P = 0.0003$, (CB/CP) $P = 0.5464$; Appendix S1: Table S4; Fig. 2A). However, the "cape x year" interaction showed some fine-scale differences between the Southern and Central Capes. The mean difference in maximum length of *H. sessile* individuals between the Southern and Central Capes increased throughout the years. In 2016, Southern Cape individuals were 2.37 ± 2.75 cm shorter on average than those at the Central Cape (LSM; $P = 0.3946$; Appendix S1: Table S4; Fig. 2A). In 2017, this difference was reversed. Average maximum length of Southern Cape individuals was 1.59 ± 2.75 cm longer than those at the Central Cape (LSM; $P = 0.5666$; Appendix S1: Table S4; Fig. 2A), and with an even wider gap in 2018 (i.e., Southern Cape individuals were 5.51 ± 2.75 cm longer) (LSM; $P = 0.0529$; Appendix S1: Table S4; Fig. 2A). Sites within the Northern and Southern Capes (Boiler Bay and Fogarty Creek; Cape Blanco North and Rocky Point, respectively) showed similar patterns to their respective cape-scale averages (Fig. 2B). However, the sites within the Central Cape (Yachats Beach and Strawberry Hill) showed opposite trends (Fig. 2B).

With respect to environmental variables, maximum length of *H. sessile* was positively correlated with Chl-a, DIN, BEUTI, and NPGO and negatively correlated with SST, SAT, MEI and SWHT (Pearson correlation; $P < 0.0001$; Appendix S1: Table S5; Fig. 3A).

Density: *H. sessile* generally increased in number of individuals per 0.25 m^2 from 2016 to 2018 at all capes (LSM; $P < 0.0001$; Appendix S1: Table S3, S4; Fig. 2C, D). Density was highest at the Northern Cape (CF) with an average of 8 ± 0.56 individuals per 0.25 m^2 (LSM; (CF/CP) $P = 0.0557$, (CF/CB) $P = 0.0476$; Appendix S1: Table S4; Fig. 2C). Boiler Bay, a site within the cape, was the main driver of the high density (Fig. 2D). Densities were lower at both the Central (CP) and Southern Capes (CB) with average density of 4 ± 0.56 individuals per 0.25 m^2 and negligible density differences between these capes (LSM; (CB/CP) $P = 0.8537$; Appendix S1: Table S4; Fig. 2C). The sites within the Central and Southern Capes (Yachats Beach and Strawberry Hill; Cape Blanco North and Rocky Point, respectively) showed similar patterns to their respective capes (Fig. 2D).

With respect to environmental variables, *H. sessile* density was positively correlated with DIN, SST, and NPGO and negatively correlated with Chl-a, BEUTI, SAT, and MEI (Pearson correlation; $P < 0.03$; Appendix S1: Table S5; Fig. 3B).

Percent Cover: Percent cover of *H. sessile* changed in ways consistent with those seen for length and density. *H. sessile* percent cover generally increased from 2016 to 2018 at all capes (LSM; $P < 0.03$; Appendix S1: Table S3, S4; Fig. 2E, F). On average, percent cover at the Northern Cape (CF) was approximately 18 ± 5.9% greater than at the Southern Cape (CB) (LSM; (CB/CF) $P = 0.0574$; Appendix S1: Table S4; Fig. 2E), but did not differ from that at the Central Cape (CP)

(LSM; (CF/CP) $P = 0.1175$; Appendix S1: Table S4; Fig. 2E). The high percent cover at the Northern Cape was driven by Boiler Bay (Fig. 2F). Percent cover at the Central Cape did not differ from that at the Southern Cape (LSM; (CB/CP) $P = 0.4692$; Appendix S1: Table S4; Fig. 2E). *H. sessile* cover at the Southern Cape was the lowest among the capes but also increased in cover the most consistently from 2016 to 2018 (Fig. 2E). The sites within the Southern Cape (Cape Blanco North and Rocky Point) showed similar patterns to their respective cape (Fig. 2F). However, the sites within the Central Cape (Yachats Beach and Strawberry Hill) showed opposite trends (Fig. 2F).

With respect to environmental variables, percent cover of *H. sessile* was positively correlated with NPGO and negatively correlated with BEUTI, SST, SAT, MEI and SWHT (Pearson correlation; $P < 0.03$; Appendix S1: Table S5; Fig. 3C).

Growth Rate: Growth rate of *Hedophyllum sessile* differed among capes (HLMM; $F = 28.07$, $P < 0.0001$; Appendix S1: Table S6; Fig. 4A, B) but did not vary across years (HLMM; $F = 1.22$, $P = 0.3614$; Appendix S1: Table S6; Fig. 4A, B). *H. sessile* at the Southern Cape (CB) grew 0.076 ± 0.026 cm/day and 0.198 ± 0.028 cm/day longer on average than those at the Central (CP) and Northern (CF) Capes, respectively (LSM; (CB/CP) $P = 0.0045$ and (CB/CF) $P < 0.0001$; Appendix S1: Table S7; Fig. 4A). The sites within all capes showed similar patterns to their respective capes (Fig. 4B).

Elemental Composition: Elemental content in *H. sessile* varied strongly with cape and year, especially at the Central (CP) and Southern (CB) Capes. The Northern Cape (CF) exhibited negligible differences in elemental composition across the years (Fig. 5A-F). Percent Carbon

decreased at the Southern and Central Capes from 2016 to 2018 by 2.53 ± 0.43% and 0.99 ± 0.43%, respectively (LSM; (CB: 2016/2018) $P < 0.0001$, (CP: 2016/2018) $P = 0.0251$; Appendix S1: Table S8, S9; Fig. 5A). Percent Nitrogen decreased at the Southern and Central Capes from 2016 to 2018 by 0.60 ± 0.07% and 0.19 ± 0.07%, respectively (LSM; (CB: 2016/2018) $P < 0.0001$, (CP: 2016/2018) $P = 0.0104$; Appendix S1: Table S8, S9; Fig. 5C). Finally, C:N increased at Southern and Central Capes from 2016 to 2018 by 2.17 ± 0.34 and 0.78 ± 0.34, respectively (LSM; (CB: 2016/2018) $P < 0.0001$, (CP: 2016/2018) $P = 0.0290$; Appendix S1: Table S8, S19; Fig. 5E). The sites within the Northern and Southern Capes showed similar patterns to their respective capes for % Carbon, % Nitrogen and C:N (Fig. 5A, D, F). However, the sites within the Central Cape showed opposite trends (Fig. 5A, D, F).

Egregia menziesii

E. menziesii generally exhibited positive responses in the immediate year post El Niño for maximum length, percent cover, and percent rachis breakage. Like *H. sessile*, the rate and direction of these responses varied by site and cape. There was also a notable decline in some of the metrics in 2018.

Maximum Length: At all capes, maximum length of *E. menziesii* increased from 2016 to 2017 and decreased in 2018 (LSM; $P < 0.0006$; Appendix S1: Table S10, S11; Fig. 6A, B). Maximum length was highest at the Southern Cape (CB) with an average of 171.22 ± 30.06 cm (LSM; $P = 0.01$; Appendix S1: Table S11; Fig. 6A). The sites within the Northern, Central and Southern

Capes (Fogarty Creek and Boiler Bay; Yachats Beach and Strawberry Hill; Cape Blanco North and Rocky Point, respectively) showed similar patterns to their respective capes (Fig. 6B).

With respect to environmental variables, maximum length of *E. menziesii* was positively correlated with Chl-a, DIN, and BEUTI, and negatively correlated with SST, MEI, and SWHT (Pearson correlation; $P < 0.0001$; Appendix S1: Table S12; Fig. 3D).

Density: The number of *E. menziesii* individuals per 0.25 m^2 generally remained constant from 2016 to 2018 at all capes except for the Central Cape (CP) in 2018 (LSM; $P < 0.004$; Appendix S1: Table S10, S11; Fig. 6C). Density was lowest at the Southern Cape (CB) across years with an average of 0.66 ± 0.33 individuals per 0.25 m^2 (LSM; $P = 0.0038$; Appendix S1: Table S11; Fig. 6C). The sites within the Northern, Central and Southern Capes (Fogarty Creek and Boiler Bay; Strawberry Hill; Cape Blanco North and Rocky Point, respectively) showed similar patterns to their respective capes (Fig. 6D).

With respect to environmental variables, density of *E. menziesii* was positively correlated with NPGO, and negatively correlated with DIN, BEUTI, SAT, and MEI (Pearson correlation; $P < 0.05$; Appendix S1: Table S12; Fig. 3E).

Percent Cover: Percent cover of *E. menziesii* was lower in 2016 and 2018 than in 2017 (Fig. 6E, F). Cover of this kelp was approximately 41.7 ± 8% in 2016, increased to 47.3 ± 8% in 2017, and decreased to 33.7 ± 8% in 2018 (LSM; $P < 0.02$; Appendix S1: Table S10, S11; Fig. 7A, B). The sites within the Northern (CF) and Southern (CB) Capes showed similar patterns to their respective capes (Fig. 7B). However, the sites within the Central Cape (CP) showed very different patterns of abundance (Fig. 6F).

With respect to environmental variables, percent cover of *E. menziesii* was positively correlated with Chl-a and DIN, and negatively correlated with NPGO and SWHT (Pearson correlation; $P < 0.03$; Appendix S1: Table S12; Fig. 3F).

Growth Rate: Growth rate of *E. menziesii* declined over three years from 2016 to 2018 at the Central and Southern Capes, but varied little at the Northern Cape (Fig. 4C). Comparing to 2016, Central and Southern Cape individuals grew 1.98 ± 0.19 cm/day and 2.19 ± 0.15 cm/day slower in 2018, respectively (LSM; (CP: 2016/2018) $P = 0.0044$, (CB: 2016/2018) $P = 0.0013$; Appendix S1: Table S6, S7; Fig. 4C). Sites within each cape showed similar patterns to those at their respective capes (Fig. 4D).

Percent Rachis Breakage: Percent rachis breakage of *E. menziesii* was higher in 2016 and 2018 and low in 2017 for all capes (Fig. 6G). Average percent breakage in 2016 was 75.5 ± 5.8%, decreased to 35.5 ± 4.9% in 2017, and increased to 63.3 ± 4.8% in 2018 (LSM; $P < 0.02$; Appendix S1: Table S13A, B; Fig. 6G). The sites within the capes showed similar patterns to their respective capes (Fig. 6H).

Postelsia palmaeformis

P. palmaeformis performance metrics were variable with no clear patterns, potentially due to limited site replicates in the Central (CP) and Southern (CB) capes.

Maximum Frond and Stipe Length: Maximum frond length of *P. palmaeformis* exhibited similar patterns as stipe length and they varied with cape and year (cape x year interaction; HLMM; [frond length] F = 17.02, $P < 0.0001$; [stipe length] F = 62.81, $P < 0.0001$; Appendix S1: Table S14; Fig. 7A, C). Southern Cape (Cape Blanco North) was the only cape where *P. palmaeformis* increased in frond (stipe) length per 0.25 m^2. Frond and stipe lengths changed from 18.0 ± 2.94 cm (16.2 ± 4.64 cm) in 2016 to 23.8 ± 2.93 cm (25.3 ± 4.63 cm) in 2018, respectively (LSM; [frond length] $P < 0.0003$; [stipe length] $P < 0.02$; Appendix S1: Table S15; Fig. 7A, C). Sites within the Northern Cape (Depoe Bay and Fogarty Creek) showed similar patterns to their respective cape-scale averages (Fig. 7B, D).

With respect to environmental variables, maximum frond and stipe length of *P. palmaeformis* was positively correlated with Chl-a, DIN, BEUTI, and NPGO and negatively correlated with SST, SAT, MEI, and SWHT (Pearson correlation; $P < 0.03$; Appendix S1: Table S16; Fig. 3G, H).

Density: *P. palmaeformis* varied in the number of individuals per 0.25 m^2 from 2016 to 2018 at all capes (HLMM; F = 27.95; $P < 0.0001$; Appendix S1: Table S14; Fig. 7E). Density was highest at the Northern Cape (CF) with an average of 28.57 ± 7.88 individuals per 0.25 m^2 (LSM; $P = 0.0582$; Appendix S1: Table S17; Fig. 7E). Depoe Bay, a site within the cape, was the main driver of the high density (Fig. 7F). Densities were low at both the Central (CP) and Southern (CB) Capes with average density of 17.17 ± 11.04 and 12.90 ± 11.04 individuals per 0.25 m^2, respectively (LSM; (CP) $P = 0.1157$, (CB) $P = 0.1154$; Appendix S1: Table S17; Fig. 7E).

With respect to environmental variables, density of *P. palmaeformis* was positively correlated with SST and MEI, and negatively correlated with DIN and BEUTI (Pearson correlation; $P < 0.03$; Appendix S1: Table S16; Fig. 3I).

Percent Cover: Percent cover of *P. palmaeformis* decreased from 2016 to 2018 at the Northern Cape (CF), increased throughout the years at the Southern Cape (CB), and increased in 2017 and decreased in 2018 at the Central Cape (CP) (LSM; (CF: 2016/2018) $P < 0.0001$, (CB: 2016/2018) $P < 0.0001$, (CP: 2016/2018) $P = 0.0005$; Appendix S1: Table S17, S18; Fig. 7G). Among sites, cover at Fogarty Creek accounted for most of the change at the Northern Cape, decreasing more dramatically compared to Depoe Bay (Fig. 7H).

With respect to environmental variables, percent cover of *P. palmaeformis* was positively correlated with Chl-a, DIN, and BEUTI, and negatively correlated with SST, SAT, MEI, and SWHT (Pearson correlation; $P < 0.01$; Appendix S1: Table S16; Fig. 3J).

Response Trajectories

Collectively (i.e., all three species together), response trajectories of the kelp communities varied in space and time (Fig. 8). In the NMDS ordination, the optimal ordination was a 2-dimensional solution. The final ordination for NMDS had 0 instability after 81 iterations and a minimum stress of 12.583 ($P = 0.004$; Appendix S1: Table S19A). The ordination captured much of the variation of the original species performance space as indicated by high non-metric and metric fits (non-metric $R^2 = 0.996$, metric $R^2 = 0.951$; Appendix S1: Table S19A). BEUTI was highly correlated with Axis 1 with stronger upwelling to the left while DIN and MEI were

highly correlated with Axis 2 with higher MEI to the top and higher DIN to the bottom (Appendix S1: Table S19B; Fig. 8).

Response trajectories of the kelps showed clear spatial differences (Fig. 8). Each cape had a different community composition: the Northern Cape (CF) as associated with higher axis 1 scores (rightward in the NMDS plane) while the Southern Cape (CB) and Central Cape (CP) were associated with lower axis 1 scores (leftward). The Southern Cape had the highest correlation with DIN and BEUTI across months and years compared to other capes.

Response trajectories also showed temporal differences (Fig. 8). The Northern Cape and Central Cape exhibited positive response trajectories from 2016 to 2017 toward communities with higher DIN and BEUTI inputs (towards the bottom right). However, the trajectories in 2018 either partly or wholly reverted to what the communities were like in 2016. Communities reverting to 2016 configurations in 2018 were more strongly correlated with MEI and DIN. The Southern Cape exhibited a steady response trajectory. All capes exhibited monthly variation with each successive month having lower axis 2 scores (towards the bottom) and were increasingly correlated with DIN and BEUTI.

Environmental Variables

BEUTI values were generally consistent over years from 2015 to 2018, peaking in May and June 2015, and June and July in 2016-2018 (Fig. 9A). Peak intensity dipped slightly in 2016. The Southern Cape (CB) had the strongest average upwelling over the years, peaking in 2018 (Fig. 9B).

The month of peak DIN values varied by year, occurring in May 2015, July/August 2016, and September 2017. Values in 2018 were lower for March-May than in previous years (Fig. 9C). Average DIN by year varied little in overall magnitude among capes from 2015 to 2017, but began declining in 2017, reaching lows in 2018 with the Southern Cape declining the least (Fig. 9D). However, the 2018 average was limited to data collected before June 2018. June to December 2018 data were unavailable due to shutdown of lab processing during the COVID-19 pandemic.

Chl-a values were highest in 2015, peaking in June, and lowest in 2018 peaking in July (Fig. 9E). Peak Chl-a occurred in July in 2016 and August in 2017. Among capes, Chl-a levels were highest at the Central Cape (CP), next highest at the Southern Cape, and lowest at the Northern Cape (CF) (Fig. 9F).

Monthly maximum SAT and SST peaked between 2014 and 2016 for all capes with values reaching close to or over 15℃(Fig. 10, 11). Maximum SST was most variable in 2013 and maximum SAT was most variable in 2013 and 2014. Furthermore, daily mean SST for the days between October and November increased over the years in Central Oregon (Strawberry Hill) and Southern Oregon (Cape Blanco North) (Fig. 12A, B).

Discussion

The responses of intertidal kelps following the 2014-16 El Niño/MHW varied among species within the order Laminariales through space (i.e., among sites [local scales] and capes [mesoscale] along the coastline), and time (i.e., days, weeks, months and years). More

specifically, kelp population dynamics changed from year to year, and were governed strongly by local and regional environmental processes and species identity (Table 1).

Synthesis of kelp responses to environmental change

El Niño has been widely documented to have detrimental effects on kelp populations through elevated seawater temperature and reduced nutrients that hamper the survival, growth and reproduction of kelps, and via storms that physically remove the kelps (Dayton and Tegner 1984, 1990, Dayton et al. 1992, Freidenburg 2002).

Our results are generally consistent with the large body of literature on the ecological effects of El Niño and consistent with hypothesis H_1 (kelp performance would increase following the thermal events). That is, the joint arrival of the historically third-most severe El Niño event in 2015-2016 and the 2014-2016 MHW reduced the performance (percent cover, maximum length and growth rate) of *H. sessile*, (maximum length) of *E. menziesii,* and (percent cover and maximum frond and stipe lengths for CBN populations*)* of *P. palmaeformis* compared to its performance afterward. This decline was most likely due to the two expected changes driven by the thermal events, increased sea temperature and declines in DIN. For example, in 2015-16, air and water temperature increased with reduced thermal variability along the Oregon coast (Fig. 10, 11). These changes were close to or over the upper threshold of the kelps' thermal tolerance range (15℃ for *H. sessile* and *P. palmaeformis* and 18℃ for *E. menziesii*) (Dean and Jacobsen 1984, 1986, Gerard 1984, Lüning & Freshwater 2008). The 2014-16 large-scale extreme MHW in the northeastern Pacific Ocean decimated giant kelp forest ecosystems across California and Baja California, Mexico (Arafeh-Dalmau et al. 2019, Cavanaugh et al. 2019, Rogers-Bennett et

al. 2019), and we infer that this event compounded the effects of El Niño and contributed to the poor performance of Oregon's intertidal kelps (Fig. 10, 11). Thermal effects were also compounded by associated declines in DIN, which is crucial for photosynthesis and protein production for kelps, and necessary for the increased energetic demands that are associated with warmer than usual temperatures (Kremer 1980, Wheeler and North 1980, Turpin et al. 1988, Turpin 1991, Gerard 1997, Gao et al. 2013, Colvard and Helmuth 2017 and Gao et al. 2017). As shown here, in 2017 *H. sessile, E. menziesii,* and *P. palmaeformis*, numbers at Oregon sites increased, particularly at the Southern Cape. Positive temporal response patterns of these intertidal kelps were associated with cessation of thermal stress conditions and the resulting increasing availability of DIN.

Role of Upwelling. As expected from hypothesis H_2 (kelp performance would vary in space), among-cape differences in upwelling likely underpinned spatial variability in intertidal kelp performance. Upwelling-driven nitrogen enrichment can ameliorate the negative effect of high temperature on macroalgae by boosting their photosynthesis and growth rates (Colvard and Helmuth 2016, Gouvêa et al. 2017, Fernandez et al. 2020). Because upwelling is stronger at the Southern than at the Central and Northern Capes, we suggest the likely higher levels of nutrients resulting from higher coastal upwelling allowed kelps to respond more quickly after the El Niño event in terms of growth rate and maximum length. This interpretation is consistent with hypothesis H_3 (higher DIN would facilitate faster recovery). However, in contrast to these measures of performance, and not consistent with H_3, *H. sessile* density was much lower at the Southern and Central Capes than at the Northern Cape and *E. menziesii* density also was lower at the Southern Cape. Furthermore, *H. sessile* density responded negatively to BEUTI and Chl-a and positively to DIN, and *E. menziesii* density responded negatively to BEUTI and DIN.

Coastal upwelling also may indirectly affect kelp density by affecting phytoplankton bloom shading and altering grazing effects (e.g., Kavanaugh et al. 2009). These effects could create a recruitment bottleneck that ultimately reduced kelp density. Specifically, *H. sessile* density was negatively associated with increasing upwelling and Chl-a, and positively associated with increasing DIN. First, as has been previously documented (Kavanaugh et al. 2009), upwelled DIN stimulates phytoplankton blooms (measured using Chl-a as a proxy) thereby increasing the turbidity of the water column and shading intertidal substrata. Since light availability is one of the crucial factors affecting the survivorship of juvenile kelps (Neushul and Haxo 1963, Neushul 1981, Dayton and Tegner 1984, Dean and Jacobsen 1984), shading from phytoplankton blooms likely negatively affected the kelp. Second, upwelled DIN may tighten the recruitment bottleneck further by stimulating the growth of juvenile kelps, which through bottom-up effects may lead to increased grazing intensity by mollusks (Menge et al. 1999, Worm et al. 2000). Thus, we hypothesize that upwelling-induced shading and grazing reduced sporeling survivorship, ultimately reducing adult density of *H. sessile* at the Southern and Central Capes.

On the other hand, *E. menziesii* density was not strongly correlated with Chl-a but was negatively correlated with upwelling and DIN. The mechanisms behind these density responses are unclear. Potential explanations for the discrepancy include: (1) Herbivores (specifically, the sea urchin *Strongylocentrotus purpuratus*) preferentially graze on adult *E. menziesii* so the grazing could physically remove the adult individuals (Van Alstyne et al. 1999, Van Alstyne et al. 2001), and (2) instead of grazing directly on adults, other herbivores (e.g., limpets) could graze on kelp spores (Jernakoff 1983). Both explanations involve a possible indirect effect of upwelling-induced grazing on *E. menziesii* individuals, ultimately contributing to a lower density at the Southern cape.

Despite the positive temporal responses of *H. sessile* in the years post-El Niño/MHW, its growth rate and %N tissue content declined in 2018 (contributing to an increase in C:N). A possible explanation is that dissolved inorganic nitrogen levels (DIN) declined in coastal waters. Despite the lack of DIN data in the later months of 2018, one could infer from Chl-a levels that DIN levels were low. N tissue content in *H. sessile* generally mirrored the DIN decline at all sites, but %N was much lower in Southern Cape individuals. Although coastal upwelling activity near the Southern Cape increased in 2018, DIN levels did not proportionally increase. These paradoxical changes could point to the possible depression of the thermocline as a result of warming, thereby inhibiting coastal upwelling from reaching the colder, more nutrient rich waters (Behrenfeld et al. 2006, Wang et al. 2015).

Declining performance in 2018 also was observed in *E. menziesii* and *P. palmaeformis*. In 2018, *E. menziesii* had low percent cover, maximum length, high rachis breakage, and low growth rate, and *P. palmaeformis* had low percent cover and maximum frond and stipe length. Essentially, in 2018 kelp communities either partially or wholly reverted to metrics that occurred in 2016. The responses of these three intertidal kelps post-El Niño/MHW highlight the potential importance of dissolved inorganic nitrogen in promoting kelps' resilience to environmental forcing.

Despite the clear responses of *H. sessile* (and the muted responses of *E. menziesii*) to El Niño/MHW, *P. palmaeformis* did not exhibit any distinct responses following these thermal events. Paine (1986) found that the 1982-83 El Niño had no effects on the recruitment, mortality, or growth of *P. palmaeformis.* Our results align with Paine's findings with the exception of maximum frond and stipe length in the Cape Blanco North population. This population was the only one that responded positively post-El Niño/MHW, a result that may be explained by high

DIN availability in the region. Percent cover and density responses of the sea palm were unclear and warrant further investigation of *P. palmaeformis* ecophysiology. Furthermore, *P. palmaeformis* density was not correlated strongly with any environmental variable, indicating other processes may be important. *P. palmaeformis* is an annual species with short distance dispersal and a high population turnover rate, which means density responses may be more dependent upon recruitment variability in space and time mediated by seasonal and episodic wave-related disturbances and cleared spaces in mussel beds (Dayton 1973, Paine 1988, Blanchette 1996, Paine et al. 2017). Thus, in general, and consistent with hypothesis H_4 (responses would vary among taxa), aspects of each species' response were idiosyncratic while others tended to be similar (Table 1).

Which metric(s) to use?

Ecologists use several metrics to characterize community structure and measure changes in community composition and species abundance. Percent cover is one of, if not the most, commonly used metrics in spatial ecology. More often than not, ecologists default to percent cover to assess responses of a species or a community to external stimuli. As we argue below, this metric is useful in some contexts, but can be problematic in others.

Like most organisms, kelps presumably optimize trade-offs between the demographic traits of growth, reproduction, and survival throughout their life history (Schiel and Foster 2006). Environmental factors have critical interactions with these traits, causing the traits to form upper and lower tolerance limits (van den Hoek 1982). We suggest that the density metric can serve as a proxy for algal population survival, and that maximum length and growth rate metrics are

proxies for growth. Assuming so, our results indicate that the demographic traits of three intertidal kelp species responded differently to the El Niño and MHW events, and to regional and local processes.

Density responses were variable across species. *H. sessile* density, and *E. menziesii* to a lesser degree, was more strongly correlated with local temperature (SAT) and light/grazing. *P. palmaeformis* density was not correlated strongly with any of the environmental variables and might be more dependent upon recruitment variability. Maximum length for all species was influenced more strongly by regional temperature (as reflected in the MEI), nutrients (DIN and BEUTI) and wave action (SWHT). El Niño weakly affected kelp density but strongly affected growth rate and maximum length.

Although maximum length and growth rate may be auto-correlated, they can provide different perspectives. For example, maximum length is a longer-term temporal, cumulative record of growth (i.e., an index of growth increments accumulated during the growth season) and the growth rate is shorter-term temporal record (i.e., growth increments vary on a daily basis). This reality might help explain some of the variation in results of growth and maximum length measurements. At the Southern Cape, *H. sessile* growth rate was lower in 2016 and 2018, while maximum length continued to increase from 2016 to 2018 with the slope decreasing slightly from 2017 to 2018. Furthermore, Southern Cape and Strawberry Hill individuals had similar maximum lengths but the growth rate was higher at the Southern Cape. The differential responses of these two metrics indicate that length patterns likely were reflective of the cumulative records of growth rate and environmental forcing during the time period (e.g., wave action and the associated frond breakage).

Another source of variability likely arises from differences among life history stages of kelps (i.e., gametophytes and sporophytes, juveniles vs. adults). Each stage experiences different ecological processes and likely differ more in risk level from some processes than others, thereby affecting the density metric. For instance, juvenile *H. sessile* are more prone to isopod *Idotea wosnesenskii* grazing than the adults, and adult *H. sessile* and *E. menziesii* are more prone to urchin *Strongylocentrotus purpuratus* and snail *Tegula funebralis* grazing than the juveniles (Van Alstyne et al. 1999, Van Alstyne et al. 2001). The larger the kelp, the more it benefits from grazing because grazing removes light-intercepting epibionts from the fronds (D'Antonio 1985, Duffy 1990) and reduces abundance of the surrounding macroalgal competitors (Duffy and Hay 2000), thereby reducing shading.

Like maximum length, we argue that percent cover integrates across environmental forcing and density and maximum length responses. Because percent cover reflects a species' demographic traits of growth and survival, it can mask internal trade-offs, which are crucial to understanding the species' responses to their environment. For example, since *H. sessile* is a fairly short (e.g., maximum height ~50-75 cm) intertidal kelp that is readily sampled using 0.25 m^2 quadrats, density and length of the kelp will weigh similarly in contributing to percent cover of the kelp. The same is true for intertidal kelps having 3-D structure like *P. palmaeformis*, i.e., density and stipe/frond length will have similar weight in measures of percent cover. However, for long intertidal kelps like *E. menziesii* (~10-15 m), length will have a much greater weight in abundance metrics than density and might skew the kelp cover.

Thus, we suggest that percent cover is a useful metric in assessing overall changes of a species or a community, but may not yield useful information if we want to understand *how* species change in response to external stimuli. Instead of the conventional use of percent cover

as a catch-all metric, ecologists should critically consider their questions of interest and evaluate whether percent cover is an appropriate single metric for estimation of changes in performance response to environmental variables.

Impacts of Environmental Forcing

Our findings revealed a complex interplay between spatial, temporal, and biological factors that modified the effects of El Niño and MHWs on intertidal kelp populations along the Oregon coast. Although our results generally agreed with prior literature on the detrimental effects of El Niño on kelp populations, these effects can be mitigated or amplified by environmental processes and kelp life history strategies. For example, coastal upwelling may provide regional relief for the kelp populations with respect to their growth needs and mitigate the adverse effects of El Niño. On the other hand, coastal upwelling may amplify, or compound, the detrimental effects of El Niño by increasing phytoplankton-induced shading and mollusk grazing on juvenile kelps, thereby reducing their density. El Niño effects are further complicated and maybe intensified by the rise of MHWs.

El Niño events are predicted to increase in frequency under greenhouse warming (Cai et al. 2018), as are MHWs (Frolicher et al. 2018). The impacts of such events on coastal environments in the short-term likely mimic those of climate change in the long-term (e.g., Menge et al. 2008, 2009). Therefore, ecological responses to El Niños and MHWs may serve as a proxy for possible long-term ecological responses to an increasingly variable climate.

The Oregon coast has been warming in recent years, especially southward (Fig. 12A, B). Historically, kelps do not perform well with short-term warming but kelp thermal plasticity may

be enhanced with nutrient inputs, thus alleviating thermal stress (Fernández et al. 2020). Therefore, we can expect kelp performance to worsen with long-term exposure to a warming climate with the possible exception of areas with high nutrients. While growth of kelps appears more dependent upon environmental forcing, survival seems more dependent upon interactions with other species (i.e., phytoplankton [light competition] and mollusks [grazing]) and kelp life history strategies (i.e., recruitment). Research shows that, depending on species and geographic location, phytoplankton and mollusks also are subjected to thermal stress and such stress may diminish their performance if the stressor exceeds their thermal limit (Thompson et al. 2004, Thomas et al. 2012, Harvey et al. 2013, Sampaio et al. 2017, Gao et al. 2018). With sufficient protection from heat and desiccation, juvenile kelps may be released from recruitment bottlenecks. However, in lab experiments, kelp recruitment success generally decreased with rising water temperatures coupled with low nutrients (Muth et al. 2019). These conflicting potential consequences make it unclear whether or not limited DIN or recruitment bottlenecks/thermal-induced recruitment failure will become more important for kelps in future warming scenarios.

Yet another scenario is that persistent warming, due to intensifying climate change exerted at least in part by ENSOs and MHWs, may cause changes in sea level and tidal ranges. In the United States, tide gauge data (going as far back as the 1930s) show either significant increasing or decreasing trends in diurnal or mean tide range (Flick et al. 2003). The exact mechanisms causing these trends are unknown but several studies suggested that changes in sea level and atmospheric conditions may have some effect (Jay 2009, Müller 2011, Müller et al. 2011). However, the effect of sea level rise on tidal amplitudes primarily depends on depth, friction, and geometry of the seaward boundary (Cai et al. 2012). Tidal records along the Oregon

coast show that extreme high sea levels in the winter were associated with strong El Niños (Komar et al. 2011) and that sea level is steadily rising along the coast (Montillet et al. 2018). Increasing variability in water level through space and time may compound the negative effect of warming on intertidal kelps by exposing them to longer and/or more variable durations of warmer than usual air and water temperature.

Conclusion

Intertidal kelp responses vary among species, across space, and through time. Moreover, each species respond differently depending on their demographic traits and life history stages. Given the greater uncertainty associated with climate change in the California Current Upwelling System and its biological implications, the findings from this study reiterate the importance of acquiring better insight into how context-specific underlying conditions modify ecosystem processes. More specifically, understanding how each demographic trait and life history stage of kelps change with biological interactions and environmental forcing over temporal and spatial scales are crucial to anticipating future climate change ramifications.

Acknowledgements

We are grateful to the many people who assisted with collecting and entering kelp survey data (H. Anderson, A. Baker-Gibbs, K. Bauer, M. Britsch, S. Choi, N. Fowler, M. Houghton, S. Hwang, J. Khakee, K. Kraus, D. Kropf, J. Merle, C. Ollier, M. Richards, M. Petit, B. Poirson, R. Postl, J. Robinson, P. Spiecker, R. Spiecker, J. Sullivan-Stack, J. Terpak, G. Thibaudat, A.

Williams and A. Wooten), and accessing and compiling environmental data (M. Frenock and J. Sapp). Discussions with F. Chan, A. Milligan and M. Behrenfeld and members of the Menge-Lubchenco lab at Oregon State University were of particular help in developing the ideas presented in this manuscript. Funding for this study was provided by Incight Scholarship, Gallaudet University Graduate Fellowship, Port Orford Research Development Fund, and Hatfield Marine Science Center's Mamie Markham Research Award to BJS, and grants from NSF (OCE1735911, DEB 1050694, DEB 1554702), the David and Lucile Packard Foundation, and the Wayne and Gladys Valley Foundation (BAM).

Literature Cited

Arafeh-Dalmau, N., Schoeman, D. S., Montaño-Moctezuma, G., Micheli, F., Rogers-Bennett, L., Olguin-Jacobson, C., and Possingham, H. P. 2020. Marine heat waves threaten kelp forests. Science 367:635-635.

Blanchette, C. A. 1996. Seasonal patterns of disturbance influence recruitment of the sea palm, Postelsia palmaeformis. Journal of Experimental Marine Biology and Ecology 197(1):1-14.

Behrenfeld, M., R. O'Malley, D. Siegel, C. McClain, J. Sarmiento, G. Feldman, ... E. Boss. 2006. Climate-driven trends in contemporary ocean productivity. Nature 444:752-755.

Cai, H., H. H. Savenije, and M. Toffolon. 2012. A new analytical framework for assessing the effect of sea-level rise and dredging on tidal damping in estuaries. Journal of Geophysical Research: Oceans 117(C9):1-20.

Cai, W., G. Wang, B. Dewitte, L. Wu, A. Santoso, K. Takahashi, Y. Yang, A. Carréric and M. J. McPhaden. 2018. Increased variability of eastern Pacific El Niño under greenhouse warming. Nature 564:201-206.

Cavanaugh, K. C., D. C. Reed, T. W. Bell, M. C. Castorani, and R. Beas-Luna. 2019. Spatial variability in the resistance and resilience of giant kelp in southern and Baja California to a multiyear heatwave. Frontiers in Marine Science 6:1-14

Cherchi, A., S. Masina, and A. Navarra. 2008. Impact of extreme CO2 levels on tropical climate: a CGCM study. Climate Dynamics 31:743–758.

Collins, M. 2000. The El Niño–Southern Oscillation in the Second Hadley Centre Coupled Model and Its Response to Greenhouse Warming. Journal of Climate 13:1299–1312.

Colvard, N., and B. Helmuth. 2017. Nutrients influence the thermal ecophysiology of an intertidal macroalga: Multiple stressors or multiple drivers. Ecological Applications 27:669–681.

D'Antionio, C. 1985. Epiphytes on the rocky intertidal red alga *Rhodomela larix* (Turner) C. Agardh: negative effects on the host and food for herbivores? Journal of Experimental Marine Biology and Ecology 86:197–218.

Davison, I. R., and G. A. Pearson. 1996. Stress tolerance in intertidal seaweeds. Journal of Phycology 32:197-211.

Dayton, P. K. 1973. Dispersion, dispersal, and persistence of the annual intertidal alga, *Postelsia palmaeformis* Ruprecht. Ecology, 54(2):433-438.

Dayton, P. K. 1985. Ecology of kelp communities. Annual review of ecology and systematics 16:215-245.

Dayton, P. K., and M. J. Tegner, M. J. 1984. Catastrophic storms, El Niño, and patch stability in a southern California kelp community. Science 224:283-285.

Dayton, P. K., and M. J. Tegner. 1990. Bottoms beneath troubled waters: benthic impacts of the 1982-1984 El Niño in the temperate zone. Elsevier oceanography series 52:433-472.

Dayton, P.K., M. J. Tegner, P. B. Edwards, and K. L. Riser. 1999. Temporal and spatial scales of kelp demography: the role of oceanographic climate. Ecological Monographs 69:219–250.

Dayton, P. K., M. J. Tegner, P. E. Parnell, and P. B. Edwards. 1992. Temporal and Spatial Patterns of Disturbance and Recovery in a Kelp Forest Community. Ecological Monographs 62:421–445.

Dayton, P. K., V. Currie, T. Gerrodette, B. D. Keller, R. Rosenthal, and D. V. Tresca. 1984. Patch dynamics and stability of some California kelp communities. Ecological monographs 54(3):253-289.

Dean, T. A., and L. E. Deysher. 1983. The effects of suspended solids and thermal discharges on kelp. The Effects of Waste Disposal on Kelp Communities. Southern California Coastal Water Research Project, Long Beach, California, 114-135.

Dean, T. A., F. R. Jacobsen. 1984. Growth of juvenile *Macrocystis pyrifera* (Laminariales) in relationship to environmental factors. Marine Biology 83:301-311.

Dean, T. A., and F. R. Jacobsen. 1986. Nutrient-limited growth of juvenile kelp, *Macrocystis pyrifera*, during the 1982- 1984 "El Nino" in southern California. Marine Biolgy 90:597-602.

DeBoer, J. A. 1981. Nutrients. In The Biology of Seawater, ed. C. S. Lobban M. J. Wynne, pp. 356-92. Berkeley: Univ. Calif. Press.

Di Lorenzo, E., N. Schneider, K. M. Cobb, K. Chhak, P. J. S. Franks, A. J. Miller, J. C. McWilliams, S. J. Bograd, H. Arango, E. Curchister, T. M. Powell, and P. Rivere. 2008. North Pacific Gyre Oscillation links ocean climate and ecosystem change. Geophysical Research Letters 35:L08607.

Doney, S. C., M. Ruckelshaus, J. E. Duffy, J. P. Barry, F. Chan, C. A. English, H. M. Galindo, J. M. Grebmeier, A. B. Hollowed, N. Knowlton, J. Polovina, N. N. Rabalais, W. J. Sydeman, and L. D. Talley. 2012. Climate change impacts on marine ecosystems. Annual Review of Marine Science 4:4.1–4.27.

Duffy, J. E. 1990. Amphipods on seaweeds: partners or pests? Oecologia 83:267–276.

Duffy, J. E., and M. E. Hay. 2000. Strong impacts of grazing amphipods on the organization of a benthic community. Ecological Monographs 70:237-263.

Ebeling, A. W., D. R. Laur, and R. J. Rowley. 1985. Severe storm disturbances and reversal of community structure in a southern California kelp forest. Marine Biology 84:287–294.

Feise, R.J. 2002. Do multiple outcome measures require p-value adjustment? BMC Medical Research Methodology 2:8.

Fernández, P. A., J. D. Gaitán-Espitia, P. P. Leal, M. Schmid, A. T. Revill, and C. L. Hurd. 2020. Nitrogen sufficiency enhances thermal tolerance in habitat-forming kelp: implications for acclimation under thermal stress. Scientific reports 10:1-12.

Filbee-Dexter, K., T. Wernberg, S. P. Grace, J. Thormar, S. Fredriksen, C. N. Narvaez, ... and K. M. Norderhaug. 2020. Marine heatwaves and the collapse of marginal North Atlantic kelp forests. Scientific reports 10:1-11.

Flick, R. E., J. F. Murray, and L. C. Ewing. 2003. Trends in United States tidal datum statistics and tide range. Journal of Waterway, Port, Coastal, and Ocean Engineering 129(4):155-164.

Freidenburg, T. 2002. Macroscale to local scale variation in rocky intertidal community structure and dynamics in relation to coastal upwelling. Ph.D. Thesis. Oregon State University.

Frölicher, T. L., E. M. Fischer, and N. Gruber. 2018. Marine heatwaves under global warming. Nature 560:360-364.

Gao, X., H. Endo, M. Nagaki, and Y. Agatsuma. 2017. Interactive effects of nutrient availability and temperature on growth and survival of different size classes of *Saccharina japonica* (Laminariales, Phaeophyceae). Phycologia 56:253–260.

Gao, X., H. Endo, K. Taniguchi, and Y. Agatsuma. 2013. Combined effects of seawater temperature and nutrient condition on growth and survival of juvenile sporophytes of the kelp *Undaria pinnatifida* (Laminariales; Phaeophyta) cultivated in northern Honshu, Japan. Journal of Applied Phycology 25:269–275.

Gao, K., Y. Zhang, and D. P. Häder. 2018. Individual and interactive effects of ocean acidification, global warming, and UV radiation on phytoplankton. Journal of Applied Phycology 30:743-759.

Gerard, V. A. 1984. Physiological effects of El Nino on giant kelp in southern California. Marine Biology Letters 5:317-322.

Gerard, V. A. 1997. The role of nitrogen nutrition in high-temperature tolerance of the kelp *Laminaria saccarina* (Chromophyta). Journal of Phycology 33:800–810.

Graham, M.H., C. Harrold, S. Lisin, K. Light, J. M. Watanabe, and M. S. Foster. 1997. Population dynamics of giant kelp *Macrocystis pyrifera* along a wave exposure gradient. Marine Ecology Progress Series 148:269–279.

Guilyardi, E. 2006. El Niño–mean state–seasonal cycle interactions in a multi-model ensemble. Climate Dynamics 26:329–348.

Gupta, A. S., M. Thomsen, J. A. Benthuysen, A. J. Hobday, E. Oliver, L. V. Alexander, ... and D. A. Smale. 2020. Drivers and impacts of the most extreme marine heatwaves events. Scientific reports 10(1):1-15.

Harley, C. D., K. M. Anderson, K. W. Demes, J. P. Jorve, R. L. Kordas, T. A. Coyle, and M. H. Graham. 2012. Effects of climate change on global seaweed communities. Journal of Phycology 48:1064-1078.

Harley, C. D., A. R. Hughes, K. M. Hultgren, B. G. Miner, C. J. Sorte, C. S. Thornber, L. F. Rodriguez, L. Tomanek and S. L. Williams. 2006. The impacts of climate change in coastal marine systems. Ecology Letters 9:228-241.

Harvey, B. P., D. Gwynn-Jones, and P. J. Moore. 2013. Meta- analysis reveals complex marine biological responses to the interactive effects of ocean acidification and warming. Ecology and Evolution 3:1016-1030.

Heaven, C., and R. Scrosati. 2004. Feeding preference of *Littorina* snails (Gastropoda) for bleached and photosynthetic tissues of the seaweed *Mazzaella parksii* (Rhodophyta). Hydrobiologia 513:239-243.

Helmuth, B., N. Mieszkowska, P. Moore, and S. J. Hawkins. 2006. Living on the edge of two changing worlds: Forecasting the responses of rocky intertidal ecosystems to climate change. Annual Review of Ecology, Evolution, and Systematics 37:373–404.

Hobday, A. J., L. V. Alexander, S. E. Perkins, D. A. Smale, S. C. Straub, E. C. Oliver, ... and T. Wernberg, T. 2016. A hierarchical approach to defining marine heatwaves. Progress in Oceanography 141:227-238.

Hoek, C. V. D. 1982. The distribution of benthic marine algae in relation to the temperature regulation of their life histories. Biological Journal of the Linnean Society 18:81-144.

Holbrook, N. M., M. W. Denny, and M. A. R. Koehl. 1991. Intertidal "trees": consequences of aggregation on the mechanical and photosynthetic properties of sea-palms *Postelsia palmaeformis* Ruprecht. Journal of Experimental Marine Biology and Ecology 146:39-67.

Hollarsmith, J. A., A. H. Buschmann, C. Camus, and E. D. Grosholz. 2020. Varying reproductive success under ocean warming and acidification across giant kelp (*Macrocystis pyrifera*) populations. Journal of Experimental Marine Biology and Ecology 522:151247.

Howard, J., E. Babji, R. Griffis, B. Helmuth, A. Himes-Cornell, P. Niemier, M. Orbach, L. Petes, S. Allen, G. Auad, … and Y. Xue. 2013. Oceans and marine resources in a changing climate. Oceanography and Marine Biology: An Annual Review 51:71–192.

IPCC. 2013. Climate Change 2013: The Physical Science Basis. Contribution of Working Group 1 to the Fifth Assessment Report of the Intergovernmental Panel on Climate Change. Cambridge University Press, Cambridge, UK and New York, USA.

IPCC. 2018. Global warming of 1.5°C. An IPCC Special Report on the impacts of global warming of 1.5°C above pre-industrial levels and related global greenhouse gas emission pathways, in the context of strengthening the global response to the threat of climate change, sustainable development, and efforts to eradicate poverty [V. Masson-Delmotte, P. Zhai, H. O. Pörtner, D. Roberts, J. Skea, P.R. Shukla, A. Pirani, W. Moufouma-Okia, C. Péan, R. Pidcock, S. Connors, J. B. R. Matthews, Y. Chen, X. Zhou, M. I. Gomis, E. Lonnoy, T. Maycock, M. Tignor, T. Waterfield (eds.)]. In Press.

Jacox, M. G., C. A. Edwards, E. L. Hazen, and S. J. Bograd. 2018. Coastal upwelling revisited: Ekman, Bakun, and improved upwelling indices for the US West Coast. Journal of Geophysical Research: Oceans 123:7332-7350.

Jay, D. A. 2009. Evolution of tidal amplitudes in the eastern Pacific Ocean. Geophysical Research Letters 36(4):1-5.

Jernakoff, P. 1983. Factors affecting the recruitment of algae in a midshore region dominated by barnacles. Journal of Experimental Marine Biology and Ecology 67(1):17-31.

Kain, J. M. 1976. The biology of *Laminaria hyperborea* IX. Growth pattern of fronds. Journal of Marine Biological Association of the United Kingdom 56:603–628.

Kavanaugh, M. T., K. J. Nielsen, F. T. Chan, B. A. Menge, R. M. Letelier, and L. M. Goodrich. 2009. Experimental assessment of the effects of shade on an intertidal kelp: Do phytoplankton blooms inhibit growth of open coast macroalgae? Limnology and Oceanography 54:276–288.

Kinlan, B. P., and S. D. Gaines. 2003. Propagule dispersal in marine and terrestrial environments: a community perspective. Ecology 84:2007-2020.

Komar, P. D., J. C. Allan, and P. Ruggiero. 2011. Sea level variations along the US Pacific Northwest coast: Tectonic and climate controls. Journal of Coastal Research 27(5):808-823.

Kremer, B. P. 1980. Transversal profiles of carbon assimilation in the fronds of three Laminaria species. Marine Biolgy 59:95–103.

Larkum, A. W. D. 1986. A study of growth and primary production in *Ecklonia radiata* (C. Ag.) J. Agardh (Laminariales) at a sheltered site in Port Jackson, New South Wales. Journal of Experimental Marine Biology and Ecology 96:177–190.

Lüning, K. 1980. Critical levels of light and temperature regulating the gametogenesis of three Laminaria species (Phaeophyceae). Journal of Phycology 16:1-15.

Lüning, K., and W. Freshwater. 1988. Temperature tolerance of Northeast Pacific marine algae. Journal of Phycology 24(3):310-315.

Mann, K. H. 1971. Relation between stipe length, environment, and the taxonomic characters of Laminaria. Journal of the Fisheries Board of Canada 28:778-780.

McCune, B., and M. J. Mefford. 2016. PC-ORD. Multivariate Analysis of Ecological Data. Version 7. MjM Software, Gleneden Beach, OR, USA.

Meehl, G. A., H. Teng, and G. Branstator. 2006. Future changes of El Niño in two global coupled climate models. Climate Dynamics 26:549–566.

Menge, B. A., F. Chan, and J. Lubchenco. 2008. Response of a rocky intertidal ecosystem engineer and community dominant to climate change. Ecology Letters 11:151–162.

Menge, B. A., F. Chan, K. J. Nielsen, E. Di Lorenzo, and J. Lubchenco. 2009. Climatic variation alters supply-side ecology: impact of climate patterns on phytoplankton and mussel recruitment. Ecological Monographs 79:379–395.

Menge, B. A., B. A. Daley, J. Lubchenco, E. Sanford, E. Dahlhoff, P. M. Halpin, G. Hudson, and J. L. Burnaford. 1999. Top-down and bottom-up regulation of New Zealand rocky intertidal communities. Ecological Monographs 69:297–330.

Menge, B. A., B. A. Daley, P. A. Wheeler, and P. T. Strub. 1997. Rocky intertidal oceanography: An association between community structure and nearshore phytoplankton concentration. Limnology and Oceanography 42:57–66.

Menge, B. A., T. C. Gouhier, S. D. Hacker, F. Chan, F., and K. J. Nielsen. 2015. Are meta-ecosystems organized hierarchically? A model and test in rocky intertidal habitats. Ecological Monographs 85:213-233.

Montillet, J. P., T. I. Melbourne, and W. M. Szeliga. 2018. GPS vertical land motion corrections to sea-level rise estimates in the Pacific Northwest. Journal of Geophysical Research: Oceans 123(2):1196-1212.

Müller, M. 2011. Rapid change in semi-diurnal tides in the North Atlantic since 1980. Geophysical research letters 38(11):1-6.

Müller, M., B. K. Arbic, and J. X. Mitrovica. 2011. Secular trends in ocean tides: Observations and model results. Journal of Geophysical Research: Oceans 116(C5):1-19.

Muth, A. F., M. H. Graham, C. E. Lane, and C. D. Harley. 2019. Recruitment tolerance to increased temperature present across multiple kelp clades. Ecology 100(3): 1-7.

Neushul, M. 1981. The domestication and cultivation of California macroalgae. Proceedings of the International Seaweed Symposium 10:71-96.

Merryfield, W. J. 2006. Changes to ENSO under CO2 doubling in a multimodel ensemble. Journal of Climate 19:4009–4027.

Neushul, M., and F. T. Haxo. 1963. Studies on the giant kelp, *Macrocystis*. Growth of young plants. American Journal of Botany 50:349-353.

North, W. 1983. Separating the effects of temperature and nutrients. The Effects of Waste Disposal on Kelp Communities, Southern California Coastal Water Research Project, Long Beach, California, 243-255.

Oliver, E. C., M. G. Donat, M. T. Burrows, P. J. Moore, D. A. Smale, L. V. Alexander, ... and T. Wernberg. 2018. Longer and more frequent marine heatwaves over the past century. Nature communications 9:1-12.

Paine, R. T. 1986. Benthic community—water column coupling during the 1982-1983 El Niño. Are community changes at high latitudes attributable to cause or coincidence? Limnology and Oceanography 31(2):351-360.

Paine, R. T. 1988. Habitat suitability and local population persistence of the sea palm *Postelsia palmaeformis*. Ecology 69(6):1787-1794.

Paine, R. T., E. R. Buhle, S. A. Levin, and P. Kareiva. 2017. Short-range dispersal maintains a volatile marine metapopulation: the brown alga *Postelsia palmaeformis*. Ecology 98:1560-1573.

Parnell, P.E., E. F. Miller, C. E. Lennert-Cody, P. K. Dayton, M. L. Carter, and T. D. Stebbins. 2010. The response of giant kelp (*Macrocystis pyrifera*) in southern California to low-frequency climate forcing. Limnology and Oceanography 55:2686–2702.

Perneger, T.V. 1998. What's wrong with Bonferroni adjustments. BMJ 316:1236-1238.

Philander, S.G.H. 1983. El Nino southern oscillation phenomena. Nature 302:295-301.

Phillips, B. F., and M. Pérez-Ramírez (Eds.). 2017. Climate Change Impacts on Fisheries and Aquaculture, 2 Volumes: A Global Analysis (Vol. 1). John Wiley & Sons.

Reed, D. C., and M. S. Foster. 1984. The effects of canopy shadings on algal recruitment and growth in a giant kelp forest. Ecology 65:937-948.

Rogers-Bennett, L., C. A. Catton. 2019. Marine heat wave and multiple stressors tip bull kelp forest to sea urchin barrens. Scientific Reports 9:1-9.

Román, M., S. Román, E. Vázquez, J. Troncoso, and C. Olabarria. 2020. Heatwaves during low tide are critical for the physiological performance of intertidal macroalgae under global warming scenarios. Scientific reports 10(1):1-14.

Rothman, K.J. 1990. No adjustments are needed for multiple comparisons. Epidemiology 43-46.

Sagarin, R. D., J. P. Barry, S. E. Gilman, and C. H. Baxter. 1999. Climate-related change in an intertidal community over short and long time scales. Ecological Monographs 69:465–490.

Sampaio, E., I. F. Rodil, F. Vaz-Pinto, A. Fernández, and F. Arenas. 2017. Interaction strength between different grazers and macroalgae mediated by ocean acidification over warming gradients. Marine Environmental Research 125:25-33.

Schiel, D. R., and M. S. Foster. 2006. The population biology of large brown seaweeds: ecological consequences of multiphase life histories in dynamic coastal environments. Annual Review of Ecology, Evolution, and Systematics 37:343-372.

Schiel, D. R., & M. S. Foster. 2015. The biology and ecology of giant kelp forests. University of California Press.

Spiecker, B. J., & B. A. Menge. 2021. El Niño and marine heatwaves: Ecological impacts on Oregon rocky intertidal kelp communities at local to regional scales. Dryad, Dataset, https://doi.org/10.25349/D9360J.

Taylor, D. I., and D. R. Schiel. 2010. Algal populations controlled by fish herbivory across a wave exposure gradient on southern temperate shores. Ecology 91:201-211.

Taylor, R. B., E. Sotka, and M. E. Hay. 2002. Tissue-specific induction of herbivore resistance: seaweed response to amphipod grazing. Oecologia 132:68-76.

Tegner, M. J. and P. K. Dayton. 1987. El Niño effects on southern California kelp forest communities. Advances in Ecological Research 17:243–279.

Thomas, M. K., C. T. Kremer, C. A. Klausmeier, and E. Litchman. 2012. A global pattern of thermal adaptation in marine phytoplankton. Science 338:1085-1088.

Thomsen, M. S., L. Mondardini, T. Alestra, S. Gerrity, L. Tait, P. M. South, ... and D. R. Schiel. 2019. Local extinction of bull kelp (*Durvillaea* spp.) due to a marine heatwave. Frontiers in Marine Science 6:1-10.

Thompson, R. C., T. A. Norton, and S. J. Hawkins. 2004. Physical stress and biological control regulate the producer–consumer balance in intertidal biofilms. Ecology 85:1372-1382.

Turpin, D. 1991. Effects of inorganic N availability on algal photosynthesis and carbon metabolism. Journal of Phycology. 27:14–20.

Turpin, E. R., G. Birch, G. Weger, and J. Holmes. 1988. Interactions between photosynthesis, respiration, and nitrogen assimilation in microalgae. Canadian Journal of Botany 66:2083–2097.

Van Alstyne, K. L., J. M. Ehlig and S. L. Whitman, 1999. Feeding preference for juvenile and adult algae depend on algal stage and herbivore species. Marine Ecology Progress Series 180:179–185.

Van Alstyne, K. L., S. L. Whitman and J. M. Ehlig, 2001. Differences in herbivore preferences, phlorotannin production, and nutritional quality between juvenile and adult tissues from marine brown algae. Marine Biology 139:201–210.

Vecchi, G. A., and A. T. Wittenberg. 2010. El Niño and our future climate: where do we stand? Wiley Interdisciplinary Reviews: Climate Change 1:260–270.

Vinueza, L. R., G. M. Branch, M. L. Branch, and R. H. Bustamante. 2006. Top-down Herbivory and Bottom-up El Niño Effects on Galápagos Rocky-Shore Communities. Ecological Monographs 76:111–131.

Wang, D., T. Gouhier, B. Menge, A. Ganguly. 2015. Intensification and spatial homogenization of coastal upwelling under climate change. Nature 518:390-394.

Watson, D. C. and T. A. Norton, 1985. Dietary preferences of the common periwinkle, *Littorina littorea* (L.). Journal of Experimental Marine Biology and Ecology 88:193–211.

Wernberg, T., S. Bennett, R. C. Babcock, T. De Bettignies, K. Cure, M. Depczynski, ... and S. Wilson. 2016. Climate-driven regime shift of a temperate marine ecosystem. Science 353(6295):169-172.

Wheeler, P., and W. North. 1980. Effect of nitrogen supply on nitrogen content and growth rate of juvenile *Macrocystis pyrifera* (Phaeophyta) sporophytes. Journal of Phycology 16:577–582.

Worm, B., H. K. Lotze, and U. Sommer. 2000. Coastal food web structure, carbon storage, and nitrogen retention regulated by consumer pressure and nutrient loading. Limnology and Oceanography 45:339–349.

Table 1. Summarized performance responses of each intertidal kelp species from 2016 to 2018.

Metric	Species		
	Hedophyllum sessile	***Egregia menziesii***	***Postelsia palmaeformis***
Maximum Length	**INCREASE**	**INCREASE** (notable decline in 2018)	**INCREASE** (only for the Cape Blanco North populations)
Density	**INCREASE**	**CONSTANT**	**VARIABLE**
Percent Cover	**INCREASE**	**DECREASE** (notable decline in 2018)	**INCREASE** (only for the Cape Blanco North populations)
Growth Rate	**INCREASE** (notable decline in 2018)	**DECREASE**	
% Rachis Breakage		**INCREASE** (notable increase in 2018)	
% Carbon	**DECREASE**		
% Nitrogen	**DECREASE**		
Carbon:Nitrogen	**INCREASE**		

Figure 1. Map of the seven study sites along the Oregon Coast.

Figure 2. *Hedophyllum sessile* performance metrics. (A) Average maximum length (centimeters per 0.25 m^2) by cape and (B) site. (C) Average density (number of individuals per 0.25 m^2) by cape and (D) site. (E) Average percent cover (% per 0.25 m^2) by cape and (F) site. All values are arithmetic mean ± standard error. For panels A, C and E: Capes are: Northern Cape Foulweather (CF) = red dot dash, Central Cape Perpetua (CP) = green dash, and Southern Cape Blanco (CB) = blue solid. For panels B, D and F: Sites are: Fogarty Creek (FC) = red solid, Boiler Bay (BB) = red dot dash, Yachats Beach (YB) = green solid, Strawberry Hill (SH) = green dot dash, Cape Blanco North (CBN) = blue solid, Rocky Point (RP) = blue dot dash.

Figure 3. Pearson correlations between three intertidal kelp performance metrics and the environmental variables. Radar plots showing: (A) maximum length, (B) density, (C) percent cover of *Hedophyllum sessile*; (D) maximum length, (E) density, (F) percent cover of *Egregia menziesii*; and (G) maximum frond length, (H) maximum stipe length, (I) density, (J) percent cover of *P. palmaeformis*. Circles represent the Pearson correlation coefficient between the species performance metric and environment variables (closed circles = $P < 0.05$ and open circles = $P > 0.05$). The position of the circle along the radial axis indicates the strength of correlation between that species performance metric and a given environmental variable. The solid black line represents zero correlation and the region inside (outside) this line represents negative (positive) correlations. Abbreviations of the environmental variables are: Chlorophyll-a (Chl-a), Dissolved Inorganic Nitrogen (DIN), Biologically Effective Upwelling Transport Index

(BEUTI), Sea Surface Temperature (SST), Surface Air Temperature (SAT), Multivariate El Niño Index (MEI), North Pacific Gyre Oscillation (NPGO), and Significant Wave Height (SWHT).

Figure 4. Growth rate of *Hedophyllum sessile* (A,B) and *Egregia menziesii* (C,D). (A,C) Average Growth Rate (centimeters per day) by cape and (B,D) by site. All values are arithmetic mean ± standard error. For panel A, capes are: Northern Cape Foulweather (CF) = red dot dash, Central Cape Perpetua (CP) = green dash, and Southern Cape Blanco (CB) = blue solid. For panel B, sites are: Fogarty Creek (FC) = red solid, Boiler Bay (BB) = red dot dash, Yachats Beach (YB) = green solid, Strawberry Hill (SH) = green dot dash, Cape Blanco North (CBN) = blue solid, and Rocky Point (RP) = blue dot dash.

Figure 5. Elemental composition of *Hedophyllum sessile* in July of each year. (A) Percent Carbon by cape and (B) site. (C) Percent Nitrogen by cape and (D) site. (E) Carbon to Nitrogen ratio by cape and (F) site. All values are arithmetic mean ± standard error. For panels A, C and E, capes are Northern Cape Foulweather (CF) = red dot dash, Central Cape Perpetua (CP) = green dash, and Southern Cape Blanco (CB) = blue solid. For panels B, D and F, sites are Fogarty Creek (FC) = red solid, Boiler Bay (BB) = red dot dash, Yachats Beach (YB) = green solid, Strawberry Hill (SH) = green dot dash, Cape Blanco North (CBN) = blue solid, and Rocky Point (RP) = blue dot dash.

Figure 6. *Egregia menziesii* performance metrics. (A) Average maximum length (centimeters per 0.25 m^2) by cape and (B) site. (C) Average density (number of individuals per 0.25 m^2) by cape and (D) site. (E) Average percent cover (% per 0.25 m^2) by cape and (F) site. (G) Average

percent breakage by cape and (H) site. All values are arithmetic mean ± standard error. For panels A, C E, and G capes are: Northern Cape Foulweather (CF) = red dot dash, Central Cape Perpetua (CP) = green dash, and Southern Cape Blanco (CB) = blue solid. For panels B, D, F and H, sites are: Fogarty Creek (FC) = red solid, Boiler Bay (BB) = red dot dash, Yachats Beach (YB) = green solid, Strawberry Hill (SH) = green dot dash, Cape Blanco North (CBN) = blue solid, and Rocky Point (RP) = blue dot dash.

Figure 7. Average percent cover of *Postelsia palmaeformis*. (A) Average maximum frond length (centimeters per 0.25 m^2) by cape and (B) site. (C) Average maximum stipe length (centimeters per 0.25 m^2) by cape and (D) site. (E) Average density (number of individuals per 0.25 m^2) by cape and (F) site. (G) Average percent cover (% per 0.25 m^2) by cape and (H) site. All values are arithmetic mean ± standard error. For panel A, C, E, and G, capes are Northern Cape Foulweather (CF) = red dot dash, Central Cape Perpetua (CP) = green dash, and Southern Cape Blanco (CB) = blue solid. For panel B, D, F, and H, sites are Fogarty Creek (FC) = red solid, Boiler Bay (BB) = red dot dash, Yachats Beach (YB) = green solid, Cape Blanco North (CBN) = blue solid.

Figure 8. Response trajectories of Oregon rocky intertidal kelp communities by month and year. Non-metric multidimensional scaling of rocky intertidal kelp communities (*Hedophyllum sessile, Egregia menziesii, Postelsia palmaeformis*) at three capes across three months (May to July) and three years (2016 to 2018). Black successional vectors connect each spatiotemporal sampling unit (sampled in the same month) through years as indicated by an arrowhead. Cape abbreviations and color are: Northern Cape Foulweather (CF) in red, Central Cape Perpetua (CP)

in green, and Southern Cape Blanco (CB) in blue. Labeled numbers represent the month and year of the survey separated by a dash. Environment parameter abbreviations are: Dissolved Inorganic Nitrogen (DIN), Multivariate El Niño Southern Oscillation Index (MEI), and Biologically Effective Upwelling Transport Index (BEUTI).

Figure 9. Upwelling, nutrient and chlorophyll-a metrics from 2015 to 2018. (A) Biologically Effective Upwelling Transport Index (BEUTI) (mmol m^{-1} s^{-1}) values by month and (B) cape from 2015 to 2018. (C) Dissolved Inorganic Nitrogen (μM) values by month and (D) cape from 2015 to 2018. (E) Chlorophyll-a (μg/L) values by month and (F) cape from 2015 to 2018. Lines represent the best fit values. For panels A, C and E, years are 2015 = red, 2016 = blue solid, 2017 = green solid, 2018 = purple solid. For panels B, D and F, capes are Northern Cape Foulweather (CF) = red solid, Central Cape Perpetua (CP) = green solid, and Southern Cape Blanco (CB) = blue solid.

Figure 10. Monthly maximum of daily surface air temperature means from 2010 to 2019. Boxplots show median (solid line) and mean (dashed line) monthly maximum surface air temperature (SAT), 25th and 75th percentiles at the edge of the boxes, 10th and 90th percentiles as whiskers, and values less than 10th percentile or greater than 90th percentile as outliers. The panels are sorted by capes: Northern Cape Foulweather (CF) = red, Central Cape Perpetua (CP) = green, and Southern Cape Blanco (CB) = blue.

Figure 11. Monthly maximum of daily sea surface temperature means from 2010 to 2019. Boxplots show median (solid line) and mean (dashed line) monthly maximum sea surface

temperature (SST), 25th and 75th percentiles at the edge of the boxes, 10th and 90th percentiles as whiskers, and values less than 10th percentile or greater than 90th percentile as outliers. The panels are sorted by capes: Northern Cape Foulweather (CF) = red, Central Cape Perpetua (CP) = green, and Southern Cape Blanco (CB) = blue.

Figure 12. Mean sea surface temperature spirals of two sites along the Oregon coast. (A) Strawberry Hill data from 1993 to 2018. (B) Cape Blanco North data from 1998 to 2018. The colored gradient bar represents mean sea surface temperature (SST in ℃). Each circle represents one year and is divided into twelve months. Blank sections represent missing data.

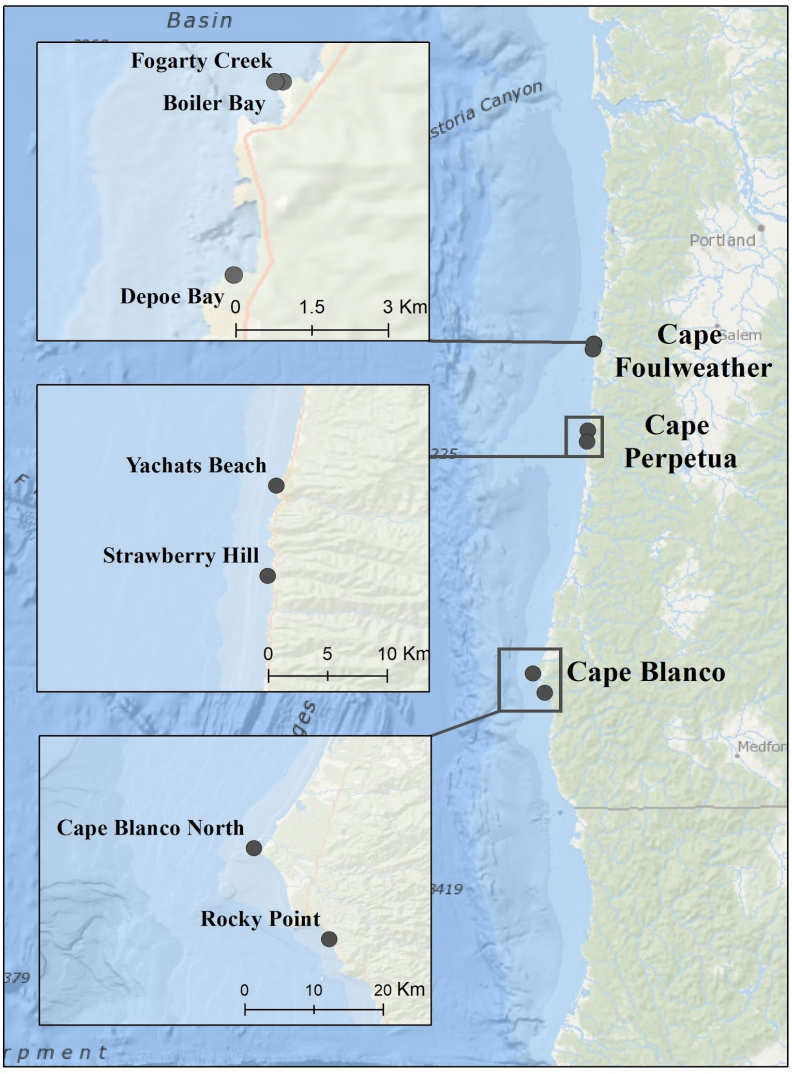

Figure 1.

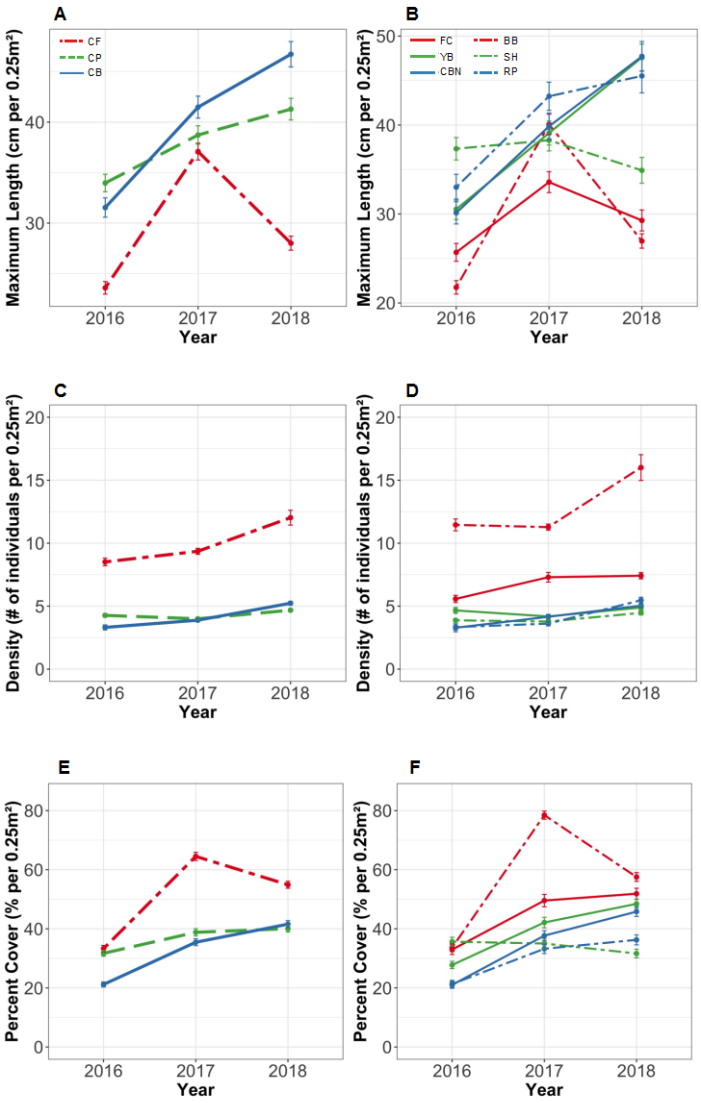

Figure 2.

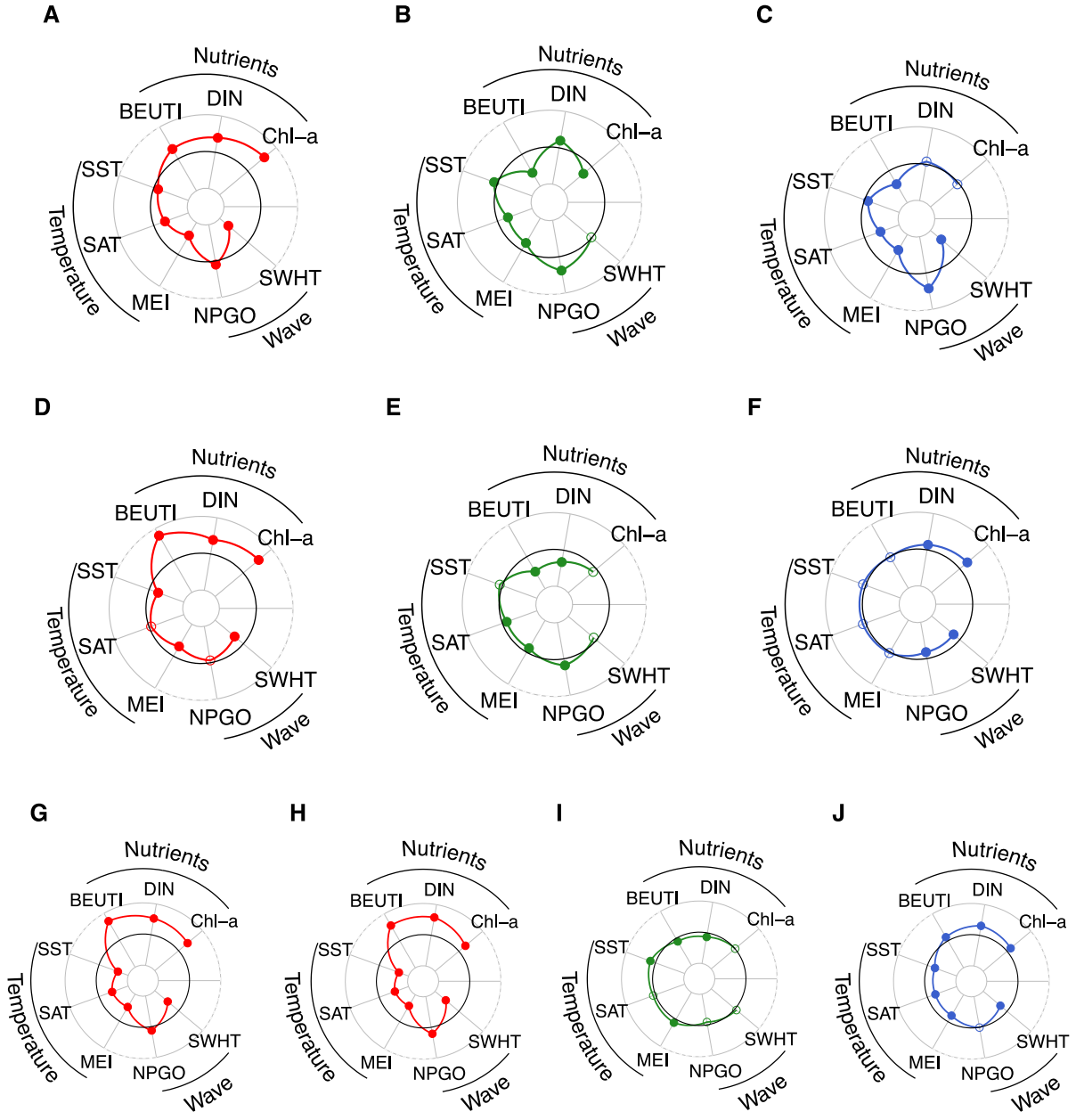

Figure 3.

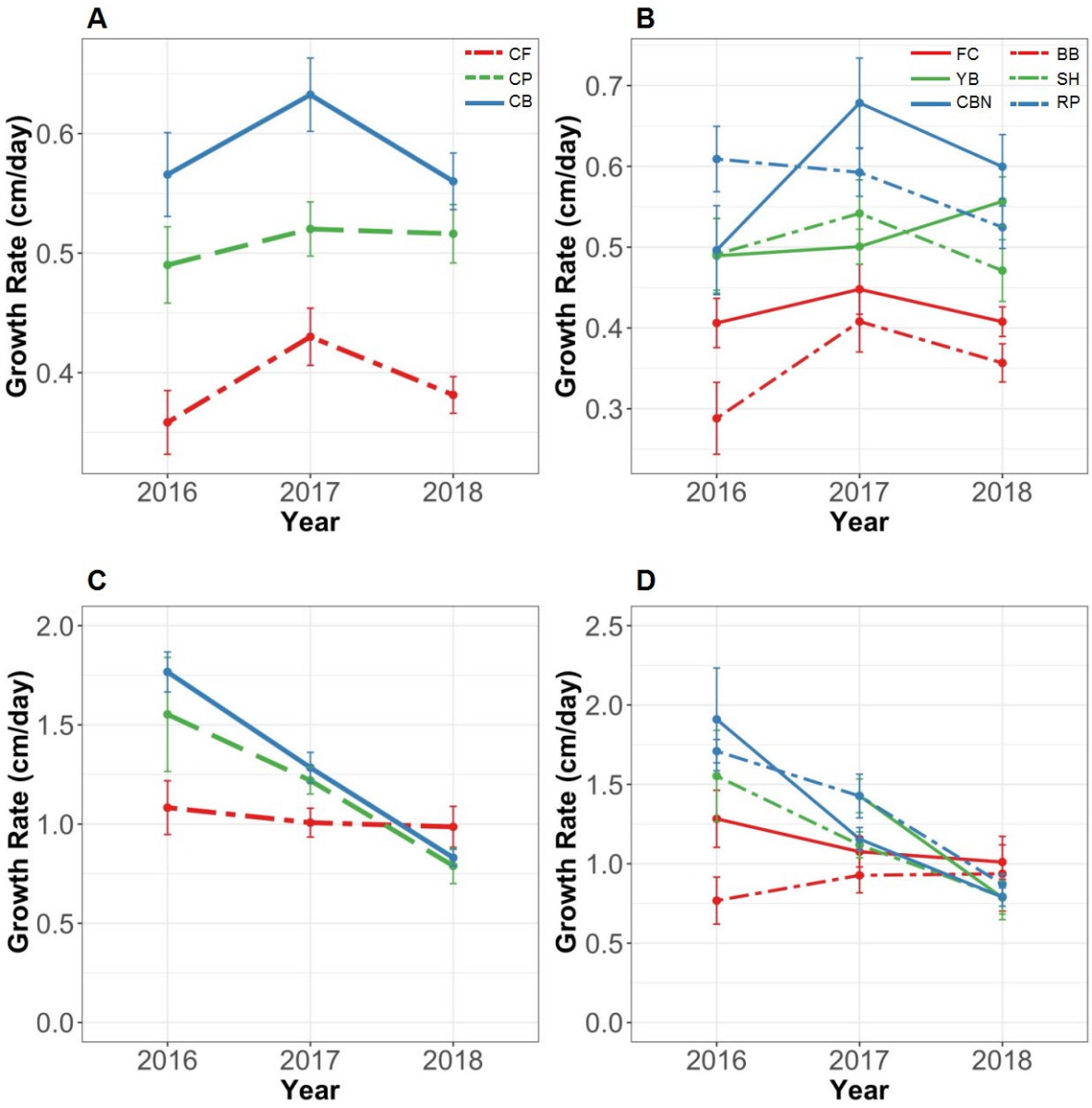

Figure 4.

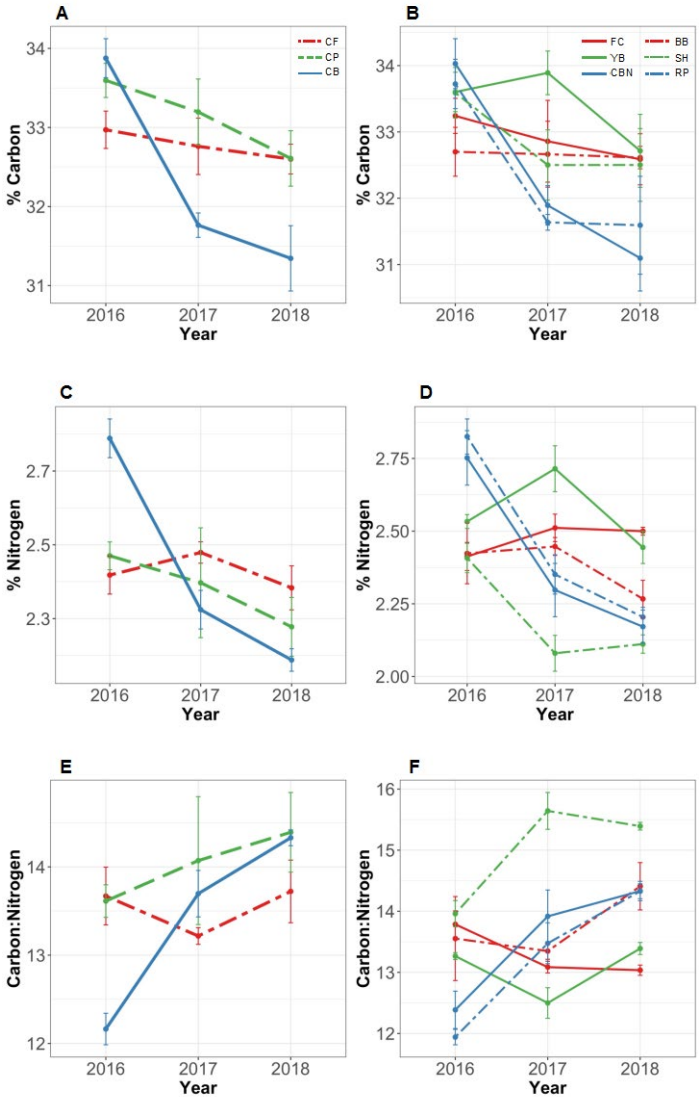

Figure 5.

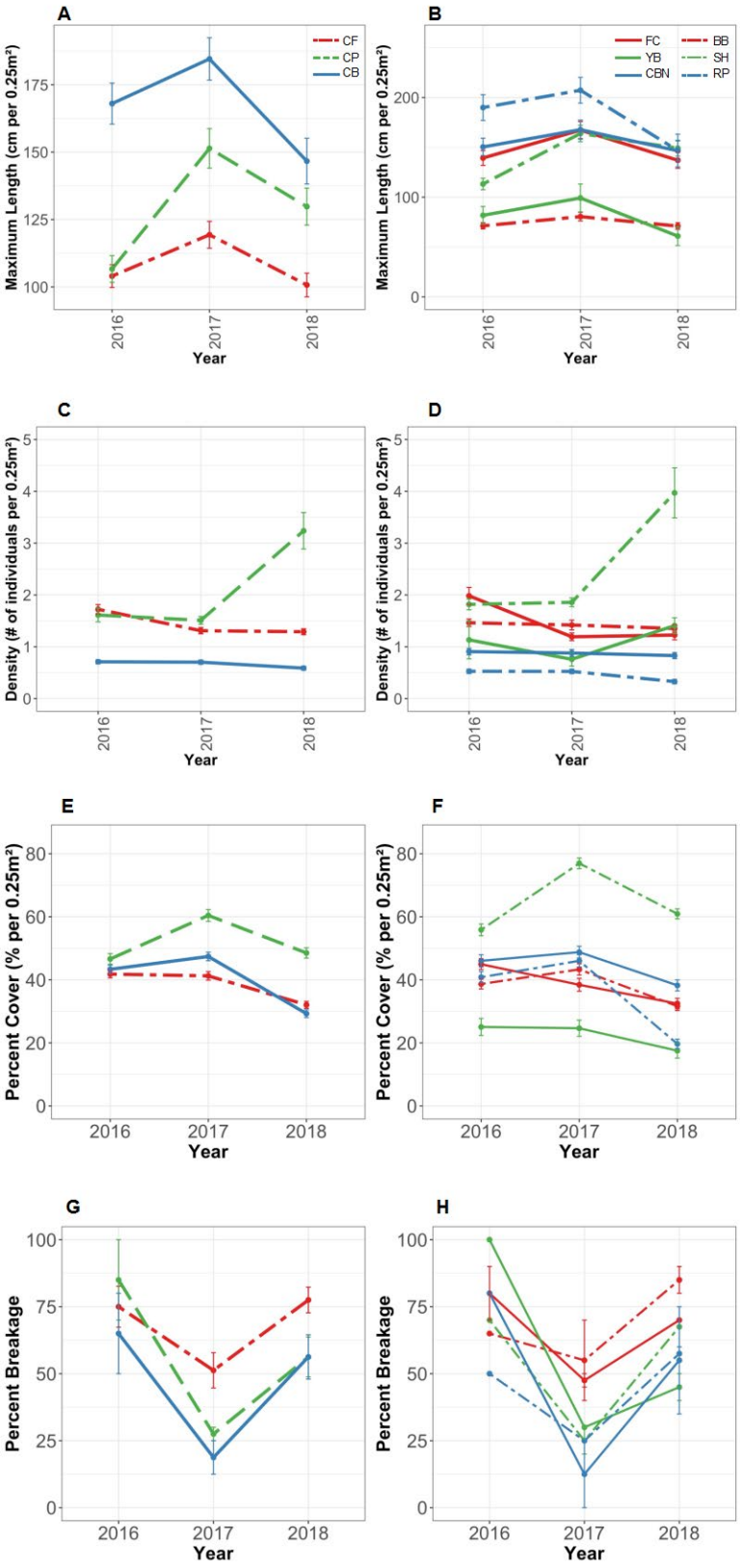

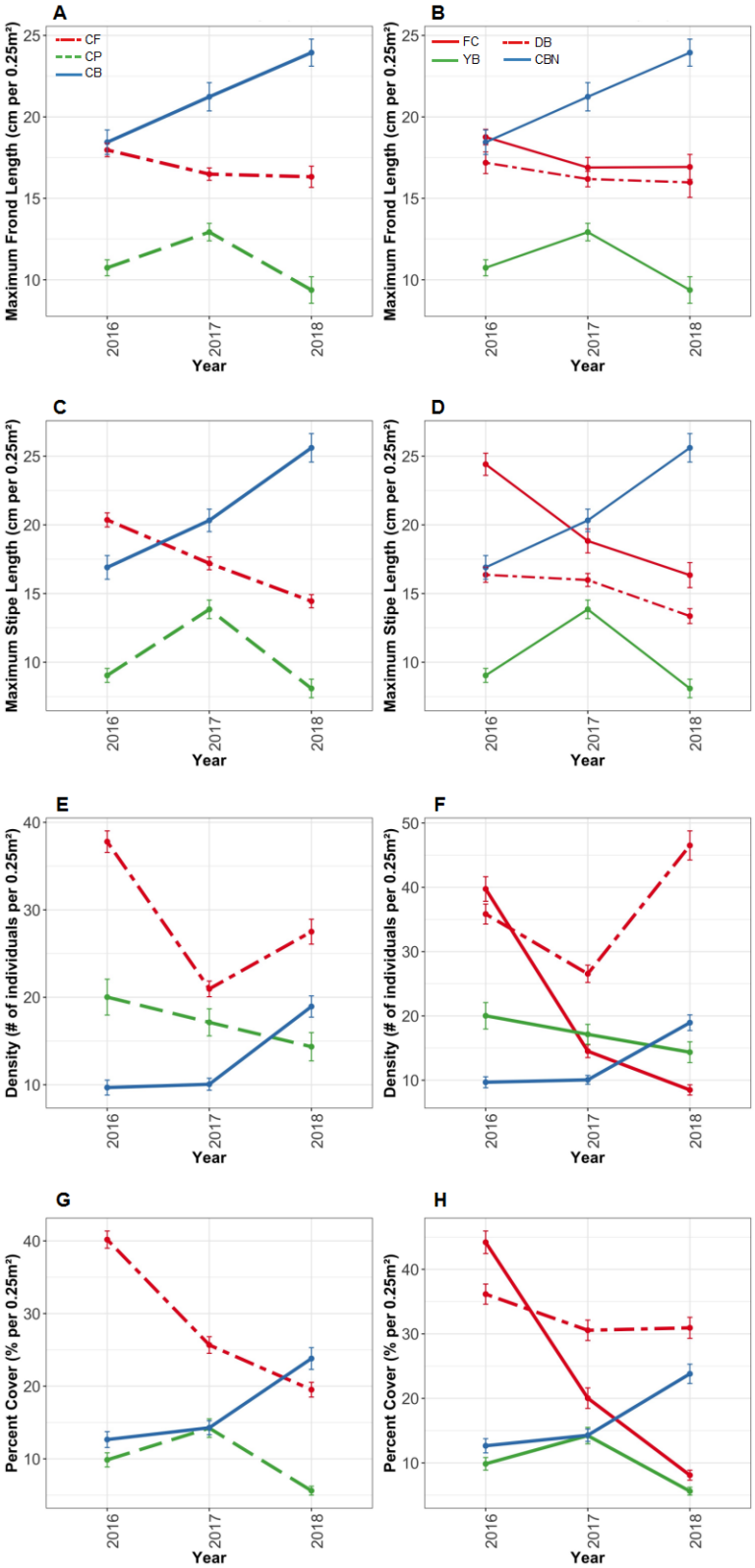

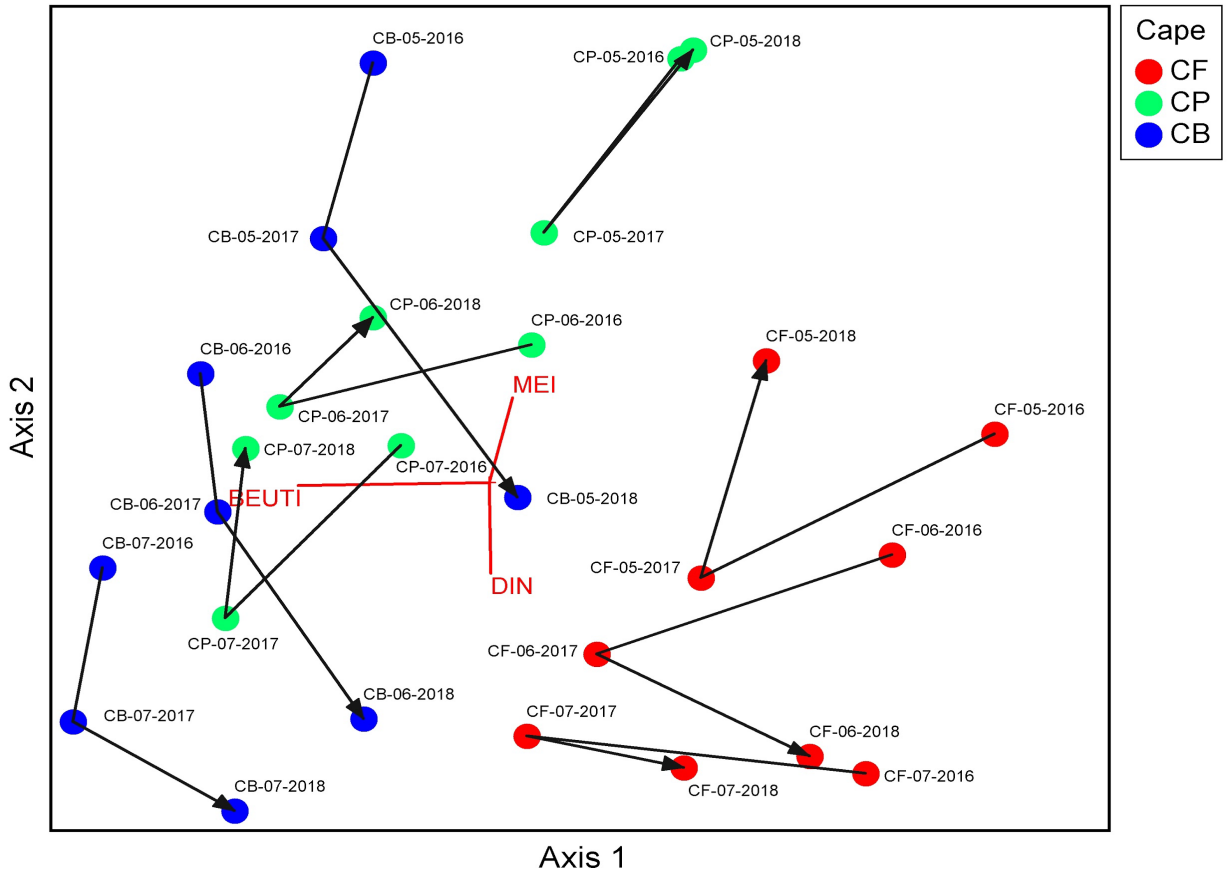

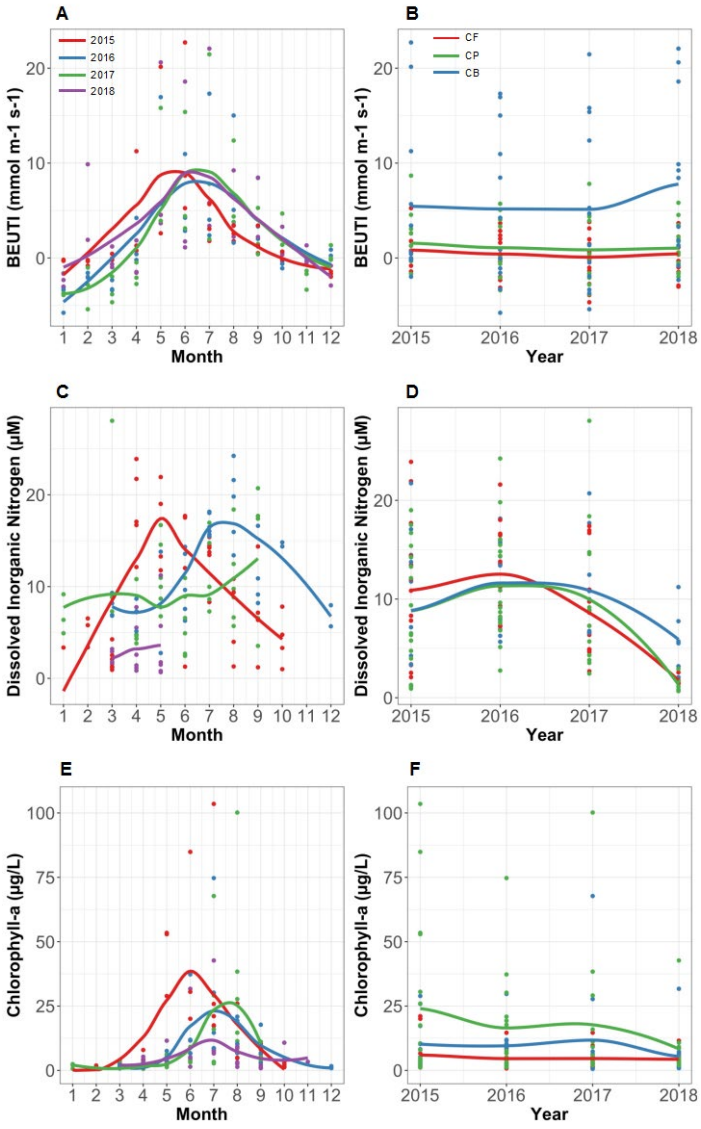

Figure 9.

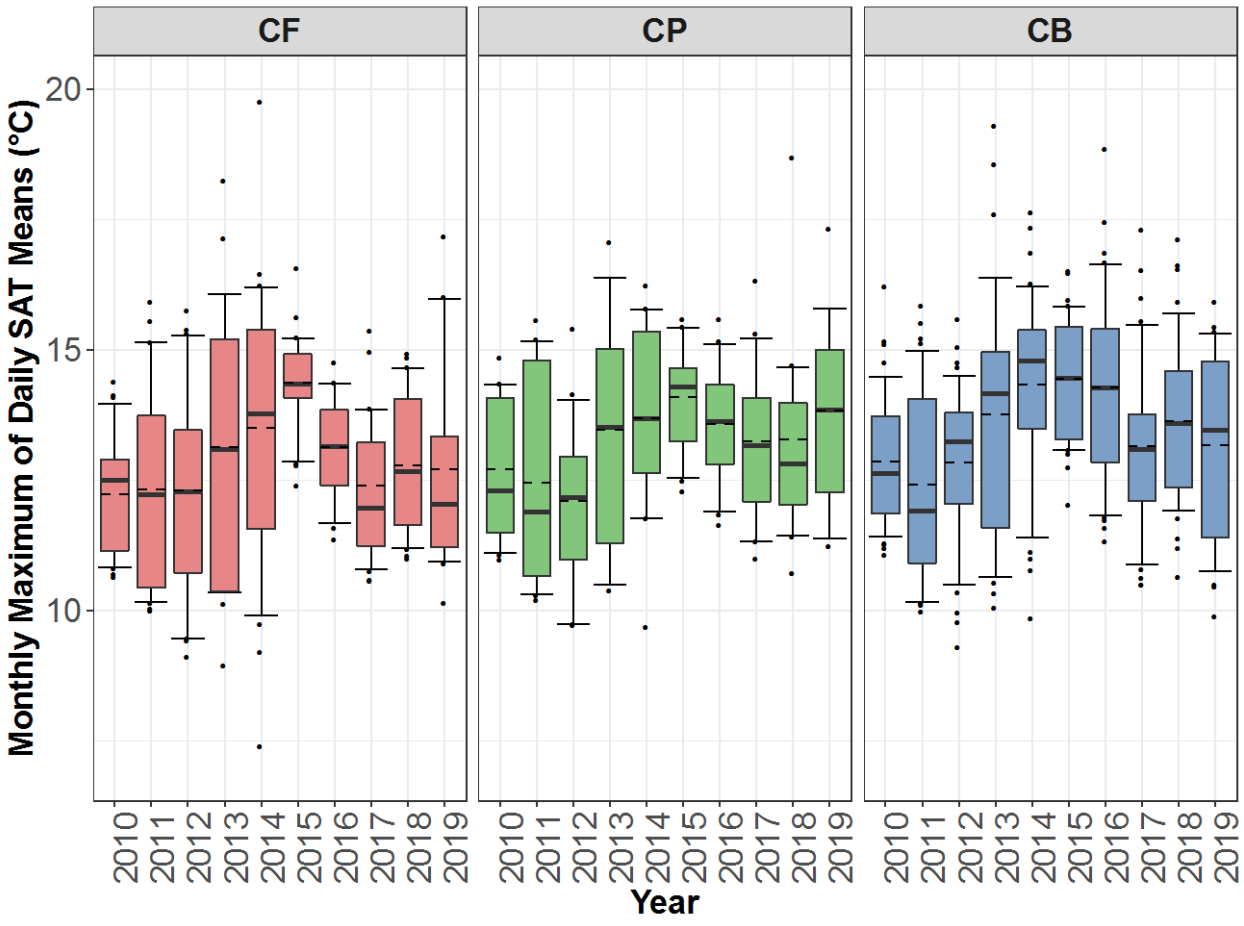

Figure 10.